

In presenting the dissertation as a partial fulfillment of the requirements for an advanced degree from the Georgia Institute of Technology, I agree that the Library of the Institution shall make it available for inspection and circulation in accordance with its regulations governing materials of this type. I agree that permission to copy from, or to publish from, this dissertation may be granted by the professor under whose direction it was written, or, in his absence, by the dean of the Graduate Division when such copying or publication is solely for scholarly purposes and does not involve potential financial gain. It is understood that any copying from, or publication of, this dissertation which involves potential financial gain will not be allowed without written permission.


A horizontal line with a vertical tick mark on the right side, followed by a handwritten signature.

SIMULATION OF A NARROWBAND
DIGITAL COMMUNICATIONS RECEIVER

A THESIS

Presented to
The Faculty of the Graduate Division
by
Walter Raymond Herbert III

In Partial Fulfillment
of the Requirements for the Degree
Master of Science in Electrical Engineering

Georgia Institute of Technology

August, 1963

6.2
12

SIMULATION OF A NARROWBAND
DIGITAL COMMUNICATIONS RECEIVER

Approved:

Dr. W. B. Jones, Jr. (Chairman)

Dr. David L. Finn

Walter B. Warren, Jr.

Date Approved by Chairman: 31 July 1963

ACKNOWLEDGMENTS

The author wishes to thank his thesis advisor, Dr. W. B. Jones, Jr., for his suggestion of the problem and for his continued guidance, assistance, and encouragement during the course of the research. Special thanks are due to the other members of the reading committee, Dr. David L. Finn and Mr. Walter B. Warren, Jr., for reviewing the manuscript and providing constructive criticisms. Appreciation is also expressed to Dr. James A. Knight, Jr. for the use of the pulse height analyzer and to Mr. James N. Hunt, Collins Radio Company, for the gift of the mechanical filter.

TABLE OF CONTENTS

	Page
ACKNOWLEDGMENTS	ii
LIST OF ILLUSTRATIONS	v
SUMMARY	viii
CHAPTER	
I. INTRODUCTION	1
II. BACKGROUND	3
Digital Communications Receivers	
Mathematical Analysis	
III. INSTRUMENTATION REQUIREMENTS	10
Equipment Approach	
General Simulation Philosophy	
Measurement of Probability Density Functions	
Simulated Receiver	
Auxiliary Equipment Required	
IV. DESIGN AND EVALUATION	17
Design	
IF Amplifier	
Timing Circuits	
Gating Circuits	
Main Input Gate	
Integrator Input Gate	
Evaluate Gate	
Integrator and Detector	
Evaluation	
Test Results	
IF Selectivity and Linearity	
Operation as Designed	
Recommendations	
V. SUMMARY AND CONCLUSIONS	25
APPENDIX	46
I. EQUIPMENT MANUAL	47

TABLE OF CONTENTS (Continued)

	Page
General Operating Procedure	
Equipment Layout	
BIBLIOGRAPHY	67

LIST OF ILLUSTRATIONS

Figure	Page
1. System Block Diagrams for Comparison of the Binary Pulse-Amplitude Modulation and the Frequency Shift Keying Receivers	30
2. Amplitude Probability Density Functions at the Output of an Envelope Detector	31
3. Output Probability Densities for the Emerson All-Gaussian System (Signal-to-Noise Ratio = 1)	32
4. Output Probability Densities for the Emerson All-Gaussian System (Signal-to-Noise Ratio = 2)	32
5. Block Diagram of Simulated Receiver and Auxiliary Equipment	33
6. Photograph of the Simulated Receiver	34
7. Schematic Diagram of the Simulated Receiver Excluding Timing Circuitry	35
8. Schematic Diagram of the Simulated Receiver Timing Circuitry	36
9. A Typical Mechanical Filter Selectivity Characteristic	37
10. Effects Upon Mechanical Filter Input Waveform by Main Gate Pulse Illustrating the "Pedestal" or "Well" Effect	19
11. Measured IF Selectivity of the Simulated Receiver	38
12. Linearity Test from the Equipment Input Through the Detector Input	39
13. Operational Configuration for the Simulated Receiver	40
14. Investigation of System Linearity	41
15. Output Probability Distribution Functions and a 100 Microsecond Integration Interval and $A_c/\sigma = 10$ db	42

LIST OF ILLUSTRATIONS (Continued)

Figure	Page
16. Output Probability Distribution Functions for a 300 Microsecond Integration Interval and $A_c/\sigma = 10$ db	43
17. Output Probability Distribution Functions for a 1.0 Millisecond Integration Interval and $A_c/\sigma = 10$ db	44
18. Output Probability Density Function for a 300 Microsecond Integration Interval and $A_c/\sigma = 10$ db	45
A1. Operational Configuration for the Simulated Receiver	51
A2. General Layout Diagram of the Simulated Receiver	52
A3. An Index of the Location and Functions of the Various Switches and Other Equipment Controls	53
A4(a). Waveform at TP 1 for a 5.0 Millisecond Main Gate Interval and a 1.20 Volt rms Input Signal	55
A4(b). Waveform at TP 2 for a 5.0 Millisecond Main Gate Interval and a 1.20 volt rms Input Signal	55
A4(c). Waveform at TP 3 for a 5.0 Millisecond Main Gate Interval and a 1.20 Volt rms Input Signal	56
A4(d). Waveform at TP 4	56
A4(e). Waveform at TP 5 with SW 2 Closed for an Integration Interval of 0.5 Millisecond and a 1.20 Volt rms Input Signal	57
A4(f). Waveform at TP 5 with SW 2 Open for an Integration Interval of 0.5 Millisecond and a 1.20 Volt rms Input Signal	57
A4(g). Waveform at TP 6 with a 5.0 Millisecond Main Gate Interval and an Input Signal of 1.20 Volts rms	58
A4(h). Waveform at TP 7 with a 5.0 Millisecond Main Gate Interval and an Input Signal of 1.20 volts rms	58
A4(i). Waveform at TP 8 for a 5.0 Millisecond Main Gate Interval	59

LIST OF ILLUSTRATIONS (Continued)

Figure	Page
A4(j). Waveform at TP 9 for a 2.25 Millisecond Begin Integrate Interval	59
A4(k). Waveform at TP 10 for a 0.5 Millisecond Integration Interval	60
A4(l). Waveform at TP 11 with No Input to the Simulated Receiver and an Integration Interval of 0.5 Millisecond. Note the Well Cancellation in the Integration Interval	60
A4(m). Waveform at TP 11 with an Input of 1.20 Volts rms and an Integration Interval of 0.5 Milliseconds . . .	61
A4(n). An Output Pulse Generated by the Simulated Receiver When Operated with a Main Gate Interval of 0.5 Milliseconds, an Integration Interval of 0.5 Milliseconds, and an Input Signal of 1.20 Volts rms . . .	61
A5. Component Layout Diagram, Circuit Board 1	62
A6. Component Layout Diagram, Circuit Board 2	63
A7. Component Layout Diagram, Circuit Board 3	64
A8. Schematic Diagram of the Simulated Receiver Excluding Timing Circuitry	65
A9. Schematic Diagram of the Simulated Receiver Timing Circuitry	66

SUMMARY

The object of the research described herein is the design, construction, and evaluation of an equipment with which an experimental investigation can be made of post-detector integration as a signal processing technique in narrowband digital communications receivers. The improvement in decoder accuracy provided by post-detector integration can be quantitatively determined from the probability distribution functions at the decoder input. Probability distribution functions can, in many cases of interest, be derived for the envelope detector output. However, similar functions have been all but impossible to obtain mathematically in closed form at the output of a post-detector integrator for receiver operation at low signal-to-noise ratios. An empirical determination of these desired post-detector distribution functions can be conveniently made using the equipment described.

Receiver selectivity and non-linearity are simulated with a mechanical filter and a conventional diode envelope detector. The mixer, local oscillator and RF amplifier are neglected. Timing and gating circuits included provide smooth, convenient control over the time interval during which modulated-carrier-pulse-noise is admitted to the equipment as well as the occurrence and duration of the time interval during which detected-modulation-pulse-noise is applied to the post-detector integrator. This allows an experimenter flexibility in performing studies of various modulation waveforms.

The equipment output is a four microsecond pulse with amplitude

proportional to the value of the integrator at the end of the integration interval. This output is designed to be compatible to a Pacific Electronics-Nuclear Company pulse height analyzer. Such an analyzer is required to be used with the simulated receiver to process a series of several thousand automatically occurring output pulses, and therefrom produce an approximation to the probability distribution functions desired.

Evaluation of the equipment designed and constructed includes the measurement of three representative probability density functions for a pulse-modulated carrier-and-noise input. Circuit diagrams of the equipment, which is completely transistorized, are included. An instruction manual detailing equipment operation and illustrating typical equipment waveforms is provided in the appendix.

CHAPTER I

INTRODUCTION

The object of the research described herein is the design, construction, and evaluation of an equipment with which an experimental investigation can be made of post-detector integration as a signal processing technique in narrowband binary digital communications receivers. A determination of the accuracy of decoding decisions in pulse receivers and, therefore, an evaluation of the improvement provided by a signal processing technique requires a knowledge of the probability distribution function at the input to the decoder. Determination of such distribution functions by a mathematical analysis of the receiver is shown to be not presently, conveniently possible, due to inherent receiver non-linearities, for receiver operation at low signal-to-noise ratios. The equipment designed consists of a simulated narrowband digital receiver, timing, switching and control circuitry.

Background information on the two most common binary pulse communication systems is presented in the second chapter. Attention is given to the similarity of the systems. The cause of and the extent of the difficulty in performing a mathematical analysis of post-detector receiver stages, of which an integrator may be considered to be one special type, is also outlined. The limited special cases in which solutions have been obtained are indicated.

System requirements are presented in the third chapter for a simulated receiver capable of being used experimentally to obtain that data

on post-detector integrators so difficult to derive mathematically. The necessity for equipment flexibility, convenience of parameter variation, and automatic operation is emphasized. A discussion of the technique proposed for the measurement of probability distribution functions using automatic analyzing and recording equipment is also included.

The fourth chapter outlines the equipment designed and its evaluation. Probability distribution and density functions measured with the equipment are included in the evaluation.

CHAPTER II

BACKGROUND

Digital Communications Receivers

The equipment described in later chapters is designed to simulate binary pulse-amplitude modulated (PAM) and frequency shift keying (FSK) digital communications receivers. Block diagrams of the respective receiver types, given in Figure 1, provide a means for comparison.

The PAM system functions as the usual superheterodyne receiver, feeding a sequence of binary pulses containing the coded information to the decision circuitry. Characteristics of this receiver important to the recognition of signals in noise are the frequency selectivity of the intermediate frequency (IF) filter, the type of envelope detector, and the method employed to make the binary decisions using the noisy signal at the detector output.

The FSK system differs primarily in that two complementary pulse sequences containing the same information are transmitted on slightly different carrier frequencies, or channels. The signals on the two channels are the inverse of one another; i.e., a pulse condition in the "mark" channel corresponds to a no-pulse condition in the "space" channel. Since there will always be a non-zero signal level in only one of the two channels, the FSK decision can be made by deciding in which of the two channels the signal most probably lies. This decision is often made by simply determining which channel has the larger output.

Decision as to the presence or absence of a receiver pulse in both the PAM system and the FSK system depends upon whether the envelope detector output exceeds or fails to exceed an appropriate amplitude threshold. How gaussian noise present in the filter output makes such a simple threshold decision uncertain can be qualitatively seen from the probability density functions of Figure 2. When random noise is present the detector output can, theoretically, assume any positive value. Non-zero probabilities exist that: (1) noise alone will exceed the decision threshold (crosshatched area of 2(c)); or (2) a signal, of amplitude A , and noise will fail to exceed it (crosshatched area of 2(d)). The probability of an erroneous indication being given in either case depends upon the signal-to-noise ratio (S/N) present.

Variation in the S/N appears in Figure 2(d) as a variation in the ratio A/δ , where A is the peak amplitude of the pulse signal alone and δ is the standard deviation of the signal with noise. Thus the probability of decision error is seen qualitatively to increase for lower S/N and decrease with higher S/N .

Several signal processing techniques may be used to improve the probability of a correct decision. The technique that will be considered here is gated post-detector integration. Instead of basing the "pulse-present" decision on one sample of the detector output, the detector output is applied to an integrator for a fixed period of time. The "pulse-present" or "pulse-not-present" decision is then made using the value of the integrator output at the end of this interval of integration. The probability of a decision error when gated post-detection integration is used is now a function of, not only the S/N , but also the occurrence

and duration of the integration interval. A quantitative mathematical expression for the probability of decision error would be helpful. Unfortunately, such an expression cannot be easily obtained.

Mathematical Analysis

If the input to a linear receiver stage is gaussian distributed, the output is gaussian distributed. Thus the statistics of a received signal as it passes through the initial linear portions of a receiver are relatively well behaved and can be calculated mathematically until the detector with its inherent non-linearity is encountered. The detector output is non-gaussian and, therefore, a mathematical analysis of succeeding stages becomes quite difficult.

Application of a single sinusoidal signal and gaussian noise through a narrowband filter to an envelope detector results in the following amplitude probability density function for the detector output^{1,2}

$$q(r) = \frac{e^{-s^2} r e^{-r^2/2N}}{N} I_0 \left(r s \sqrt{\frac{2}{N}} \right); s^2 = \frac{A_c^2}{2N} \quad (2-1)$$

where r is the random amplitude, I_0 is a Bessel function of the first kind, s^2 is the power S N ratio at the input to the detector, A_c is magnitude of the sinusoidal, pre-detector carrier, and N is the mean noise power at the input to the detector. Note that as the power signal-to-noise ratio approaches zero, the noise-only condition $q(r)$ approaches the Rayleigh

¹Mischa Schwartz, Information Transmission, Modulation and Noise, McGraw-Hill Book Company, Inc., New York, 1959, p. 400.

²David Middleton, "Some General Results in the Theory of Noise Through Non-Linear Devices," Quarterly of Applied Mathematics, Vol. 5, No. 4, pp. 470, 471, January 1948.

distribution, Figure 2(c), which is for $A_c = 0$,

$$q(r) = \frac{r}{N} e^{-r^2/2N} . \quad (2-2)$$

Also, as A_c becomes very large in comparison with N , $q(r)$ can be shown to be approximated by a gaussian function of mean, A_c ,

$$q(r) = \frac{1}{\sqrt{2\pi A_c N}} e^{-(r-A_c)^2/2N} ; \quad \begin{matrix} rA_c \gg N \\ A_c^2 \gg N \end{matrix} . \quad (2-3)$$

It is this gaussian approximation at high S/N , Figure 2(d), that makes possible conventional and straightforward analysis of post-detector stages.

Several investigators have sought to obtain an analytic expression for the output of a post-detector receiver stage operating at low S/N where the above gaussian approximation no longer holds. Such a post-detector stage is generally termed an audio or video amplifier, as would be the case in most conventional communications equipment; however, one should recall that the post-detector integrator of interest here can be considered to be a simple one-pole, low pass filter.

M. Kac and A. J. F. Siegert³ have investigated the statistical affects of uncorrelated white gaussian noise with and without signal for such an IF, square law envelope detector, and audio amplifier system. While the work is quite general with respect to both IF and audio pass-band characteristics and the form of the input signal, the final result,

³M. Kac and A. J. F. Siegert, "On the Theory of Noise in Radio Receivers with Square Law Detectors," Journal of Applied Physics, Vol. 18 No. 4, pp. 383-397, April 1947.

the amplitude probability density function at the audio output, is indicated as the Fourier transform of a rather complicated characteristic function. The results, although exact, are of limited engineering value in that the required Fourier inversion integral cannot generally be evaluated in closed form.

M. A. Meyer and David Middleton⁴ working along the same lines as Kac and Siegert show that the desired video (audio) output probability density function can be determined explicitly provided the eigenvalues of a certain integral equation can be found. For signals and noise both the eigenvalues and the associated eigenfunctions of this integral equation are needed. Moreover, only the characteristic function of the desired distribution--not its Fourier transform--is expressible in convenient form so that a practical, usable solution is no closer. However, results are included which show that the output probability distribution tends to that obtained by an infinitely wide post-detector filter (i.e., no post-detector selectivity at all) when the video filter is wide compared with the IF, and to a gaussian distribution when the final filter is narrower than the IF.

R. C. Emerson,⁵ who derives a characteristic function similar in form to that of Kac and Siegert, expands the logarithm of the characteristic function, which appears as an infinite product, in a power series. Coefficients in this series are used to obtain an asymptotic expansion for the desired probability density. Results, shown in Figures 3 and 4, are

⁴M. A. Meyer and David Middleton, "On the Distribution of Signals and Noise after Rectification and Filtering," Journal of Applied Physics, Vol. 25, No. 8, August 1954.

⁵R. C. Emerson, "First Probability Densities for Receivers with Square-Law Detectors," Journal of Applied Physics, Vol. 24, No. 9, pp. 1168-1176, September 1953.

the amplitude probability density function at the audio output, is indicated as the Fourier transform of a rather complicated characteristic function. The results, although exact, are of limited engineering value in that the required Fourier inversion integral cannot generally be evaluated in closed form.

M. A. Meyer and David Middleton⁴ working along the same lines as Kac and Siegert show that the desired video (audio) output probability density function can be determined explicitly provided the eigenvalues of a certain integral equation can be found. For signals and noise both the eigenvalues and the associated eigenfunctions of this integral equation are needed. Moreover, only the characteristic function of the desired distribution--not its Fourier transform--is expressible in convenient form so that a practical, usable solution is no closer. However, results are included which show that the output probability distribution tends to that obtained by an infinitely wide post-detector filter (i.e., no post-detector selectivity at all) when the video filter is wide compared with the IF, and to a gaussian distribution when the final filter is narrower than the IF.

R. C. Emerson,⁵ who derives a characteristic function similar in form to that of Kac and Siegert, expands the logarithm of the characteristic function, which appears as an infinite product, in a power series. Coefficients in this series are used to obtain an asymptotic expansion for the desired probability density. Results, shown in Figures 3 and 4, are

⁴M. A. Meyer and David Middleton, "On the Distribution of Signals and Noise after Rectification and Filtering," Journal of Applied Physics, Vol. 25, No. 8, August 1954.

⁵R. C. Emerson, "First Probability Densities for Receivers with Square-Law Detectors," Journal of Applied Physics, Vol. 24, No. 9, pp. 1168-1176, September 1953.

obtained under the assumption of a gaussian-shaped post-detector selectivity. The results are interesting for comparative purposes; however, they are applicable only insofar as the gaussian shape assumed represents the post-detector integrator of interest. An integrator, considered in filter terminology, is a simple single pole, low-pass filter. Emerson's gaussian assumption is very good for the audio video post-detector band-pass amplifier he was considering; however, it is not a good model for a low pass filter characteristic.

Post-detector "integration" has been studied extensively by researchers interested in the accurate reception of radar returns in the presence of noise. Unfortunately, the integration considered is actually a summation of samples of the detector output, each sample being taken from a different radar return. As the time between radar returns is relatively long, and as the radar bandwidth is quite wide,⁶ the samples taken are uncorrelated. Marcum, in a paper classic to the field,⁷ obtains expressions for the characteristic function, probability density function, and distribution function of the summation of N ($N = 1, 2, 3, \dots$) detector output samples for both the linear and the square-law envelope detectors operating on pulsed carrier and noise.

With PAM and FSK communications receivers, however, a decision must be made after only one pulse interval has elapsed. Thus, Marcum's work using N target returns is not directly applicable; however, his results

⁶David Middleton, Introduction to Statistical Communication Theory, McGraw-Hill, New York, 1960, p. 147.

⁷J. I. Marcum, "A Statistical Theory of Target Detection by Pulsed Radar: Mathematical Appendix," I.R.E. Transactions on Information Theory, April 1960.

could be applied if several uncorrelated detector output samples were considered to be taken during the one PAM or FSK pulse interval available. Such uncorrelated samples would require evaluating the detector output samples were considered to be taken during the one PAM or FSK pulse interval available. Such uncorrelated samples would require evaluating the detector output every τ seconds,⁸ where $\tau = (\text{IF Bandwidth})^{-1}$, at the zero crossing of the autocorrelation function for band-limited white noise. The relationship between the IF bandwidth and pulse duration used would, therefore, determine the number of independent samples which could be taken. Such a sampling technique might well provide a clue to an analytical, perhaps digital computer implemented, solution for the output probability density function of a post-detector integrator.

The use of several samples to represent a continuous integration is, of course, an approximation, the accuracy of which must be evaluated. Unless there are many independent samples available to represent each pulse, this verification would be difficult to do mathematically. It could be done experimentally.

⁸Middleton, Ibid.

CHAPTER III

INSTRUMENTATION REQUIREMENTS

Equipment Approach

General Simulation Philosophy

In light of the severe complications involved in obtaining a conveniently usable mathematical expression for the output of a post-detector integrator, it was decided that effort directed toward design and construction of equipment capable of yielding an empirical solution would be of value. Such an equipment--a simulated digital communications receiver--would provide an experimental means for establishing the relationship between the input signal-to-noise ratio, the interval of post-detector integration, and the amplitude probability-density function at the integrator output. From this data, the probability of decision error can be found.

To be of maximum usefulness such a simulated receiver should be as flexible as possible. Also, as it must be used to make a large number of measurements, convenience of parameter variation and automatic operation are of considerable importance. Flexibility is required in the selection of modulating signal waveform, in the signal-to-noise ratio to be applied, and in the time of occurrence and the duration of the integration interval. Variation of these parameters must be accomplished conveniently. Automatic means should be provided for evaluating the integrator at the end of the integration interval because of the very large amount of data required for the measurement of a probability density function.

Measurement of Probability Density Functions

The value of the integrator output at the end of each integration interval is one sample of a continuous random variable. The probability density function of such samples can be established by sample averaging. (The driving signal at the receiver input causing the post-detector randomness is stationary white gaussian noise.)

The probability desired is⁹

$$P(X_i < \xi < X_i + \Delta X) \quad (3-1)$$

where ξ is the random amplitude of the integrator output as sampled at the end of the integration interval, X_i is the i^{th} unit of amplitude measure, and ΔX is the incremental amplitude measure. The probability density at the i^{th} increment is then

$$\frac{1}{\Delta X} P(X_i < \xi < X_i + \Delta X) \quad (3-2)$$

and the approximate probability density function is

$$P_{\xi}(X_i) \cong \frac{1}{\Delta X} P(X_i < \xi < X_i + \Delta X), \quad i = 0, 1, 2, 3, \dots \quad (3-3)$$

The probability density function for a continuous X is defined as

$$P_{\xi}(X)dX = P(X < \xi < X + dX) . \quad (3-4)$$

The smaller the interval ΔX , the better the approximation, but in practice ΔX on the order of $1/50$ of the total range of ξ is usually sufficient.

⁹Y. W. Lee, Statistical Theory of Communication, John Wiley and Sons, Inc., New York, 1960, pp. 268-272.

Now consider a function v of ξ such that

$$v_i(\xi) = \begin{cases} 1 & \text{for } X_i < \xi < X_i + \Delta X \\ 0 & \text{elsewhere} . \end{cases} \quad (3-5)$$

The mean value of $v_i(\xi)$ is

$$\begin{aligned} \overline{v_i(\xi)} &= \int_{-\infty}^{\infty} v_i(X) P_{\xi}(X) dX \\ &= \int_{X_i}^{X_i + \Delta X} P_{\xi}(X) dX = P(X_i < \xi < X_i + \Delta X). \end{aligned} \quad (3-6)$$

Hence the approximate probability density function above (3-3) is

$$P_{\xi}(X_i) \cong \frac{1}{\Delta X} \overline{v_i(\xi)} \quad (3-7)$$

This result states that, if a unit pulse $v_i(\xi)$ is generated whenever ξ falls in the amplitude interval $(X_i, X_i + \Delta X)$, the ensemble average of these unit pulses divided by ΔX is the approximate value of the probability density of ξ , the random height of the sampled integrator output, at $X = X_i$.

Pulse height analyzers are commercially available which perform the above described amplitude quantization automatically. The machines count, through generation of a pulse output similar to $v_i(\xi)$, the number of times in a given total number of samples that the pulse amplitude falls within each of the machine's quantized amplitude levels. The relative frequency of occurrence of pulses in each level is, for a sufficiently large number of pulses, an approximation to the probability density

function desired.

A Pacific Electronics-Nuclear Co. (PENCO) pulse height analyzer operating as described above with a maximum of one hundred channel resolution is located in the Radioisotopes and Bioengineering Laboratory on the Georgia Tech campus and is available for student and faculty use upon request. The output of the simulated receiver, therefore, should be a pulse compatible to the PENCO pulse height analyzer and linearly proportional to the value of the post-detector integrator at the end of the integration interval. The desired approximate probability density function can then be automatically compiled by the PENCO equipment. PENCO equipment readout is available both in pictorial form on a cathode-ray tube and in printed form on an adding machine tape.

Simulated Receiver

A simulated receiver capable of performing the desired post-detector integrator experiments with maximum flexibility and convenience is outlined in the block diagram of Figure 5. Virtually no selectivity or non-linearity of importance here occurs in the RF, mixer, and oscillator stages of an FSK or PAM receiver. As the areas of mathematical difficulty lie in the narrowband IF filter, the detector and the integrator, the unnecessary complications of a mixer and RF stage are avoided by operating the oscillator, or simulated "carrier," shown directly at the intermediate frequency.

As was pointed out in Chapter II, approximations to the probability density functions at the output of a post-detector filter have been obtained by Emerson when the IF and post-detector filters are assumed to be gaussian. In order to expand experimentally on these results, the

the IF amplifier used in the simulated receiver should be markedly non-gaussian. Practical digital communications receivers should have excellent adjacent channel rejection (so that crosstalk between closely tuned receivers is minimized). Thus the equipment constructed should employ as close to an ideal rectangular passband characteristic as possible. Practical IF bandwidths used are on the order of 1250 cps for FSK systems and 3000 cps for PAM systems.¹⁰

The envelope detector commonly used in communications equipment depends upon the resistance characteristic of a diode for its operation,¹¹ a characteristic much nearer square-law than linear. All the investigators noted in Chapter II, with the exception of Marcum, derived their results on the assumption of a square-law envelope detector characteristic. Marcum, who was able to compare solutions for both the square-law and linear characteristics, could find no significant performance advantages of one type over the other.¹² Therefore, no advantage is seen in the simulated receiver having other than a conventional diode envelope detector.

The switching circuitry shown in Figure 5 should provide, in addition to the basic timing required for automatic operation, techniques whereby the beginning and the duration of the integration interval may be conveniently and smoothly varied. As the detected noise is uncorrelated

¹⁰Reference Data for Radio Engineers, Fourth Edition, International Telephone and Telegraph Company, 1956, p. 23.

¹¹F. E. Terman, Electronic and Radio Engineering, Fourth Edition, McGraw-Hill Book Company, Inc., New York, 1955, pp. 547-557.

¹²Marcum, Ibid., p. 189.

every τ seconds,¹³ where τ is $(\text{IF Bandwidth})^{-1}$, the integration interval with both its beginning and the duration variable over a range of 0.1τ to 10τ should allow all reasonable investigative flexibility required. A four microsecond sample of the integrator level at the end of the integration interval forms the output pulse.

The post-detector integrator employed in the simulated receiver must be capable of gated operation of from 30 microseconds to 3 milliseconds duration if the 3,000 cps PAM IF bandwidth required is assumed. Operational integration is precluded, without design of a special very wide-banded high gain amplifier, by the short gating intervals involved. Therefore, the integrator to be selected is seen as an ordinary RC integrator, which is, in effect, a one pole low-pass filter. The accuracy of integration in such types is sufficient so long as the interval of integration is a small fraction of the RC time constant.

Auxiliary Equipment Required

Equipment shown outside the dashed lines of Figure 5 is considered auxiliary, although essential, equipment and is not a portion of the simulated receiver. No modulator is included as it is expected that others will use the simulated receiver to study post-detector integration as applied to various types of pulse modulation, i.e., raised cosine, rectangular, trapezoidal, et cetera. The modulator design is felt best left to the experimenter making the modulation study.

The ready availability of oscillators of sufficient frequency stability in the 455 kc range and the requirement for an external modulator

¹³David Middleton, Introduction to Statistical Communication Theory, Ibid.

make the design and construction of an oscillator internal to the simulated receiver superfluous. Means, however, should be available (a digital counter is recommended) for monitoring the frequency of the oscillator used to assure bandcenter operation.

Facility is included within the equipment for adding the noise produced by the external gaussian noise generator to the modulated carrier. Such a gaussian white noise generator is available within the Electrical Engineering School.

The PENCO pulse height analyzer discussed earlier in this chapter and its related linear amplifiers are essential for effective use of the simulated receiver. The four micro-second random amplitude output pulse generated by the simulated receiver is first amplified so that all fluctuations of interest occur in a 4 volt to 10⁴ volt range. This amplified pulse is then fed to the pulse height analyzer from which an approximation to the probability density function is obtained as per the discussion earlier in this chapter.

CHAPTER IV

DESIGN AND EVALUATION

Design

A simulated receiver designed to perform in accordance with the specifications outlined in Chapter III is shown in Figure 6. Figures 7 and 8 are circuit diagrams of the equipment.

IF Amplifier

As the IF bandwidth used determines the time constants required for the timing circuitry, attention was first concentrated on this portion of the equipment.

A mechanical filter was seen to give a close approximation to the rectangular, steep-skirted selectivity desired with the additional advantage of simplified circuitry. The particular filter chosen has a 6 db bandwidth of 3.1 kilocycles and a bandcenter frequency of 455 kilocycles. Figure 9 shows a typical selectivity characteristic for a mechanical filter similar to that selected.

The amplifier at the input to the mechanical filter serves both as an amplifier and a gate. In the presence of the main gate pulse at the base of T2 or when SW 1 is closed, T1 is biased in its active region and acts as a regular transistor amplifier. In the absence of either of these, however, T1 is biased in its cut-off region and no input signal is allowed into the equipment. The reasons behind this arrangement are deferred to the section on gating circuits below. The output amplifier is of standard type. Both amplifiers are designed to approximately match

the 8,000 ohms input and output impedance of the mechanical filter.

Timing Circuits

Selection of the 3.1 kc IF bandwidth requires that the timing circuits controlling the beginning and duration of the integration interval be smoothly variable from 30 microseconds through 3 milliseconds. The timing multivibrators designed are standard types¹⁴ designed to incorporate variable RC time constants. Coarse time constant, and therefore pulse duration, control is exercised through the switched capacitors, each of which differs by a factor of two from that below it in size. Fine control is accomplished through the potentiometer which gives a stable time constant variation over a range slightly greater than a factor of two providing a convenient overlap between capacitor settings.

Gating Circuits

Gating circuits are used in the simulated receiver for: (1) admitting the input signals for a fixed, determinable period of time (an override switch, SW 1, Figure 7 is provided should continuous operation be desired), (2) applying the detected signal to the post-detector integrator during the desired integration interval, and (3) sampling the amplified integrated signal for the first four microseconds immediately after the integration interval to obtain the pulse output required.

Main Input Gate. The input stage to the mechanical filter serves both as amplifier and input gate. This input gate serves to admit only a known, controllable duration of input signal and is important in that it allows the operator control of the signal admitted to the equipment.

¹⁴ Leonard Strauss, Wave Generation and Shaping, McGraw-Hill Book Company, Inc., New York, 1960, Chapters 9 and 10.

Under normal conditions when the main gate pulse is not present, transistor T2 is biased into its cut-off region raising the emitter of T1 to approximately 10 volts and driving T1 into cut-off. The collector of T1 then sits at 10 volts and no input signal reaches the mechanical filter or the remainder of the equipment.

The presence of the main gate pulse drives T2 into saturation dropping its collector to just above ground potential and thereby biasing T1 into its active region. (The same effect can be accomplished by closing the normally open SW 1 switch.) However, as the main gate pulse allows T1 to become active rather than cut-off, the d.c. potential at the collector of T1 drops from 10v to its active bias point causing a waveform similar to that shown in Figure 10.

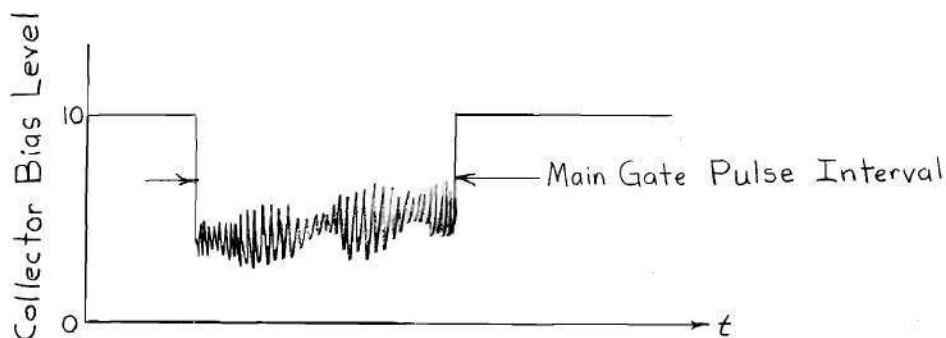


Figure 10. Effects upon Mechanical Filter Input Waveform by Main Gate Pulse Illustrating the "Pedestal" or "Well" Effect.

As will be shown during the discussion of the equipment evaluation later in this chapter, this "well" effect at the collector of T2 is of no consequence due to the relatively narrow passband of the mechanical filter as compared with the sharp fall and rise times experienced.

Integrator Input Gate. Control over the application of the detected signal to the integrator is exercised by a gating circuit composed of T5, T6, and T7. Presence of the Integrate gate pulse causes T6 to go from cut-off into saturation which in turn drives T5 from cut-off into its active region. This action is similar to that of T2 and T1 when a main gate pulse occurs. However, in order to obtain effective use of the integrator, only gated detected modulation with no well effect, as illustrated in Figure 10 for the Main Input Gate, should be applied.

The undesired well effect is offset by the action of T7. The integrate gate pulse applied to T7 does not cause a change in state but is amplified by T7 as a pulse. By adjustment of the 50K potentiometer, the height of the pulse supplied from T7 can be made to exactly cancel the well generated by the T6-T7 combination so that the input to the following stage sees the gated modulation as a positive signal of true amplitude.

Evaluate Gate. The output of the integrator is amplified and then sampled by the evaluate gate transistor, T10. The gate transistor is normally saturated so that the integrator output waveform is normally shunted to ground. During the four microsecond evaluate interval, however, T10 is cut-off and the current flows instead through the 5K potentiometer and the 12K resistor. This generates an output voltage pulse proportional to the value of the integrator at the close of the integration interval and compatible with the PENCO amplifiers and analyzer.

Integrator and Detector

The RC integrator employed in the simulated receiver is of standard configuration with the exception that provision is incorporated for switching the capacitor used. This allows the integrator time constant

to change as the length of the integration interval is varied, thereby maintaining the integrator output at approximately the same amplitude (for constant input) irrespective of the integration interval. The rotary switch wafer for C_I is located on the same shaft as the wafer used in switching the integrate multivibrator time constant. Opening switch SW 2 disrupts the integrator and changes the waveform on TP 5 from that at the output of the integrator to that being applied to the integrator.

An envelope diode detector of conventional type is used.

Evaluation

Test Results

Evaluation of the simulated receiver was accomplished, for the most part, by operating the equipment as it was designed to operate and noting the results obtained. However, preliminary tests were performed to establish the frequency selectivity characteristics and linearity of the receiver from the input terminals through the IF filter to the detector input.

IF Selectivity and Linearity. Selectivity characteristics of the IF filter were established by applying gaussian white noise from a General Radio Model 1390-B noise generator to the receiver input using a Panoramic Electronics Model SB-12b spectrum analyzer and to examine the signal present (with SW 1, closed for continuous operation) at the detector input, TP 2. Figure 11 shows on a logarithmic or decibel scale the IF selectivity characteristic present. "0" on the horizontal scale corresponds to 455.0 kc as determined by a Berkley digital counter while each horizontal interval corresponds to 500 cps.

Linearity measurements were made with a 455.0 kc input signal with the output again taken at TP 2, the detector input and with SW 1 closed for continuous operation. The results are given in Figure 12.

Operation as Designed. The major portion of the evaluation performed was with the simulated receiver connected in its operational configuration as shown in Figure 13. Unless otherwise stated, all tests were run with a 5 millisecond main gate interval and with the integration interval as given, but placed symmetrically around a point in time 2.5 milliseconds after the main gate opens.

Overall linearity from signal generator to analyzer output was first investigated by applying to the simulator a 455.0 kc "carrier" of measured amplitude. The height of the pulses analyzed (represented by the analyzer channel into which the pulse amplitude was counted) should vary directly as the input amplitude. Data obtained for integration intervals of 30 microseconds, 300 microseconds, and 3 milliseconds is presented in Figure 14. Note that the data for each integration interval has at least 0.6 volt and 50 channel region of linear operation.

The general procedure (see Instruction Manual, Appendix, for details) used to measure probability density functions with the simulated receiver was to first apply the signal without noise for a fixed period of time to aid in calibrating the analyzer and to illustrate the effects of noise, and then to apply the desired proportions of signal plus noise for a similar time or until a sufficiently smooth density function was attained. Results obtained for a peak signal to rms noise ratio, A_c/σ , of 10 db at the detector input and for integration intervals of 100 microseconds, 300 microseconds and 1 millisecond are presented as probability

distribution functions and compared with the respective signal-only data in Figures 15, 16, and 17 respectively. The 100 microsecond data is also presented as a probability density function in Figure 18.

Recommendations

Use of the simulated receiver in making the above probability density measurements uncovered equipment shortcomings which should be recognized by an experimenter using the equipment. The maximum output of the gaussian noise generator used, General Radio Model 1390-B, is such that it is impossible, due to the narrow selectivity of the IF filter, to obtain a figure for A_c/σ at the detector of smaller than 10 db without decreasing the input signal below 1.2 volts rms and thereby, causing non-linear equipment operation. Additional external amplification should be provided for the noise input.

The integrate gate and "well" effect compensation circuit comprised of T5, T6, and T7, Figure 7, exhibits a tendency to drift slightly over relatively long periods of time. An exact compensation at TP 11 for the well effect will be in error after thirty minutes of operation by a typical maximum of 10 millivolts. This small change seems insignificant compared to the size of the well without compensation. However, because of the large amount of gain and the presence of an integrator between TP 11 and the pulse height analyzer, such a change can cause as much as a ten channel analyzer shift in the signal-only condition. This drift is not overly serious, however, as sufficient data for an acceptable probability distribution function can be obtained from 5,000 samples corresponding to approximately ten minutes operating time. Nevertheless, it is recommended that a signal-only test be made both before and after the

signal-plus-noise data is taken to assure that negligible drift occurred.

CHAPTER V

SUMMARY AND CONCLUSIONS

Design, construction and evaluation of an equipment capable of simulating receivers used in PAM and FSK systems is the subject of this research. The simulated receiver was designed to provide a convenient means whereby experimental data could be gathered on the advantages of post-detector integration when applied to pulse communications systems.

An explanation of the similarity between PAM and FSK communications systems which allows a single equipment to simulate both types is explained in the beginning of the second chapter. The chapter goes on to illustrate the threshold decision technique used in such binary digital communications systems, how the technique depends upon a knowledge of the probability density function at the decision point, and the effect of unavoidable random noise on the density functions and the decisions resulting therefrom.

As post-detector integration, i.e., integrating the detector output before making the decision as to whether a pulse was present or not during the preceding interval, is thought to provide an increase in decision reliability, consideration was given to the signal statistics with and without noise at the detector output, the input to a post-detector integrator. With post-detector integration, however, the pulse present decision is deferred to the integrator output and a knowledge of the probability density functions there is now required.

A survey of the literature indicates that the probability density

function at the output of any post-detector filter, of which the integrator may be considered to be very simple, low-pass type, is quite difficult to determine. One researcher, Emerson, was able to obtain a solution to the problem, but only under assumptions not wholly compatible with post-detector integration. In light of these mathematical difficulties, an experimental approach to the problem was felt to be of value. Design, construction and evaluation of an equipment capable of providing the data required by such an experimental approach is the subject of this thesis.

Design requirements for the equipment were outlined in Chapter III. Briefly, the equipment must simulate the narrowband IF and diode detector characteristics of actual FSK and PAM receivers and incorporate gating and timing circuits to allow flexible, convenient control of that portion of the input signal applied to the post-detector integrator. A technique must be included for evaluating the integrator at the end of the integration interval and processing the values obtained over a large number of samples so that a probability density function can be measured. The theory of probability density function measurement is presented in Chapter II.

A description of the equipment designed to fulfill the requirements set forth is included, together with an equipment evaluation, in Chapter IV. The simulated receiver is completely transistorized and uses a Collins mechanical filter, which has 3.1 kc bandwidth centered on 455 kc, to attain the desired, non-gaussian IF selectivity. A conventional diode envelope detector is employed ahead of the gated RC integrator.

Timing and gating circuitry comprises a considerable portion of

the equipment. An input gate, in addition to the gate controlling the integrator, is provided so that the experimenter may, if desired, exercise control over the duration of the input signal admitted to the equipment. A switch is provided to disable the input gating and thereby provide the continuous operation necessary to a detector input signal-to-noise ratio determination. The input gate is seen to be of particular importance to an investigator making a study of various pulse modulation signals in conjunction with post-detector integration.

Multivibrators are used to control the timing of the equipment. Three of these employ variable RC time constants so that the length of input signal admitted, the interval between the time the input signal starts and the integrate gate opens, and the length of time during which the integrate gate remains open may all be conveniently varied. A fixed, timing astable multivibrator is incorporated so that the main signal gate will open automatically every 150 milliseconds to admit the desired interval of signal. At the end of the integration interval, a fixed four microsecond pulse is generated which triggers the sampling circuit to evaluate the integrator and produce a four microsecond output pulse proportional to the integrator value.

Output pulses from the simulated receiver are applied to an external linear pulse amplifier and then to a pulse height analyzer. The analyzer, which is able to resolve one hundred amplitude levels, determines the level into which each incoming pulse falls. As an automatic count is kept of the total number of pulses occurring in each equally spaced amplitude quantization interval, the readout from the analyzer after several thousand pulses have been applied is an approximation to the

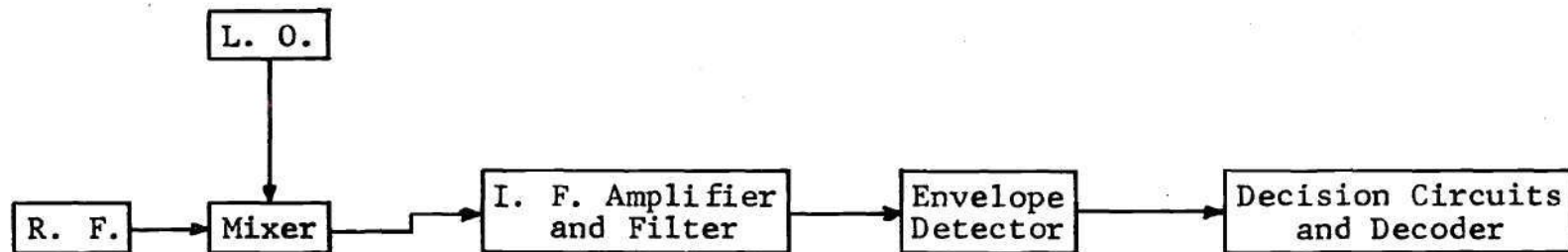
probability density function of the input pulses, i.e., the integrator amplitude at the end of the integration interval.

Linear evaluation of the equipment from the input through to pulse height analyzer shows a region of linear operation over approximately 0.6 volt at the input or 50 channels at the pulse height analyzer regardless of the duration of the integration interval used. To assure that the equipment would, indeed, perform as designed, probability density measurements were made with integration intervals of 100 microseconds, 300 microseconds and 1 millisecond and a detector peak signal to rms noise ratio, A_c / σ , of 10 db.

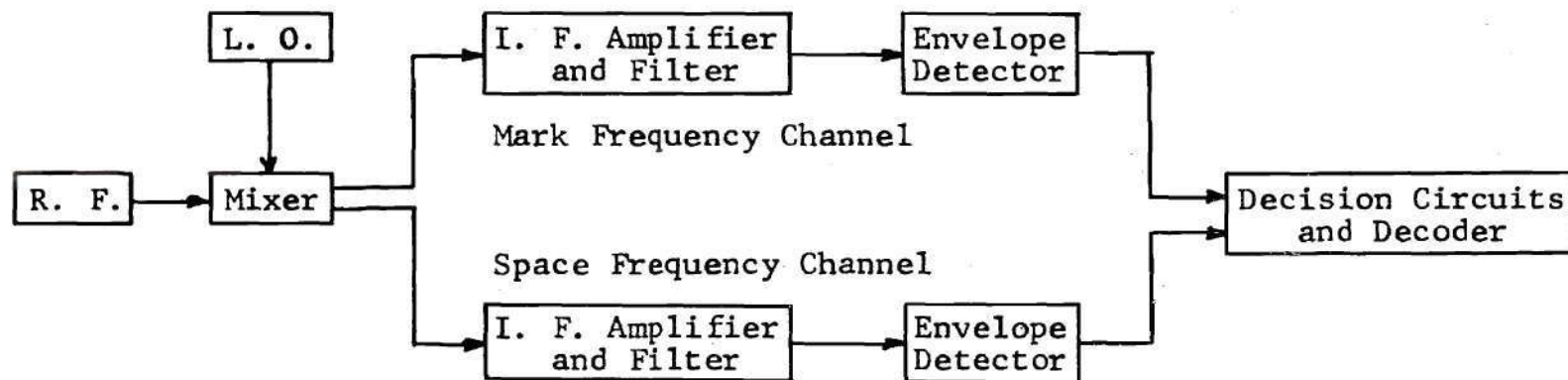
Two unanticipated equipment shortcomings were encountered in the equipment evaluation. The noise generator output was seen to be insufficient to force sufficient power through the narrow 3.1 kc IF bandwidth to provide as wide a variety of A_c / σ values as would be required for an extensive probability density function investigation. Additional external noise amplification is recommended. Slight drift was discovered at a critical place in the receiver's operation. Fortunately, however, it is sufficiently slow in occurring that operation is not curtailed if data is not taken for longer than ten minutes, or approximately 5,000 output pulses. This was seen to be sufficient in the measurements made.

As is probably true with research in any area, regions of interest are seen which time and scope prohibit exploring. The most obvious here is that of a modulation waveform study, the logical next step with the simulated receiver and the purpose behind its being constructed. Does post-detector integration offer more advantage with, say, raised cosine or triangular modulation waveforms? Threshold criteria for detection

of pulse signals in noise, a subject in itself, could be investigated using probability density functions obtained with the simulated receiver.



(a) Binary Pulse-Amplitude Modulation Receiver.



(b) Frequency Shift Keying Receiver.

Figure 1. System Block Diagrams for Comparison of the Binary Pulse-Amplitude Modulation and the Frequency Shift Keying Receivers.

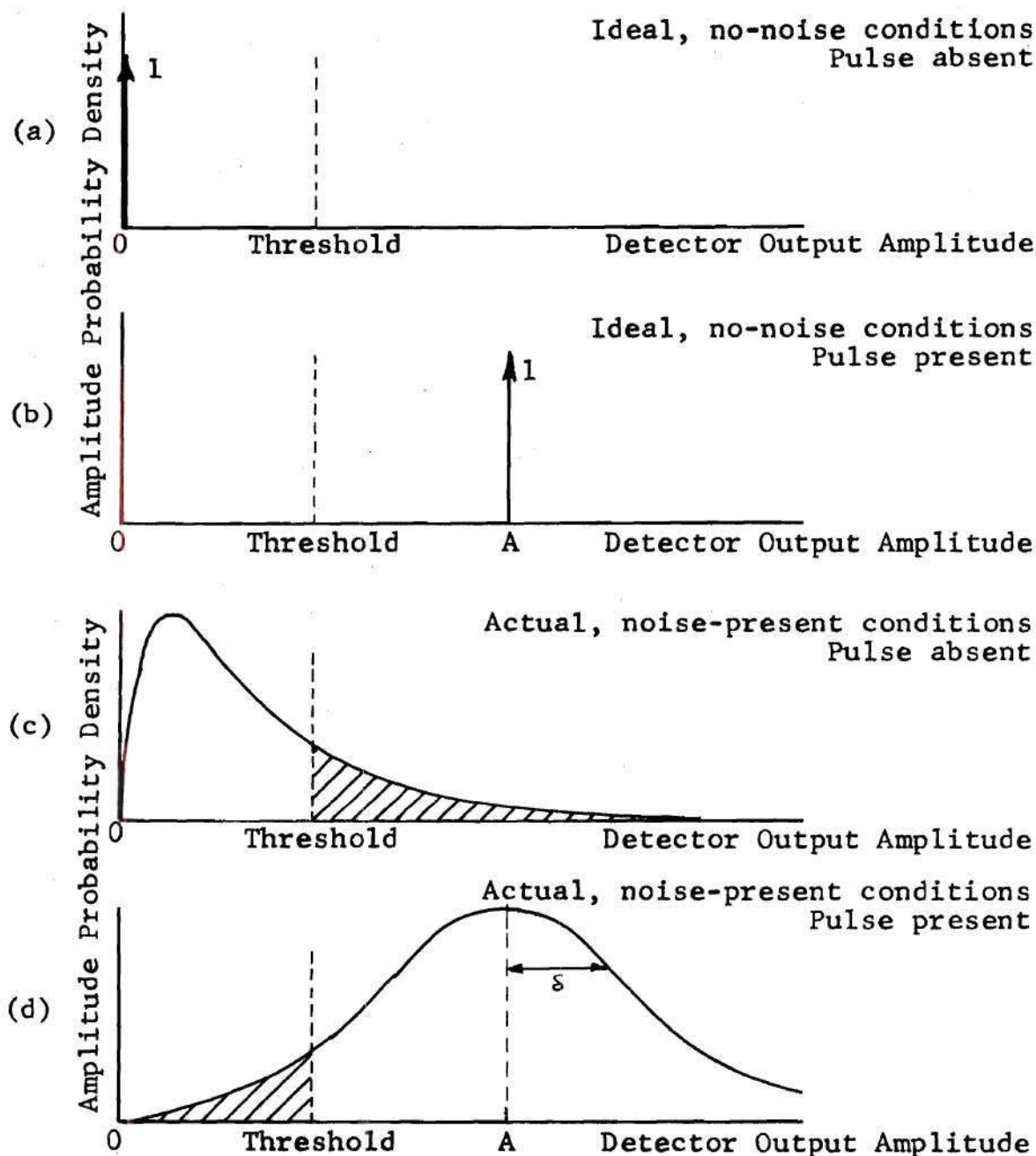


Figure 2. Amplitude Probability Density Functions at the Output of An Envelope Detector. Note in (a) and (b) that the Output is Certain, Whereas in (c) and (d) the Presence of Noise Causes an Uncertainty to Exist.

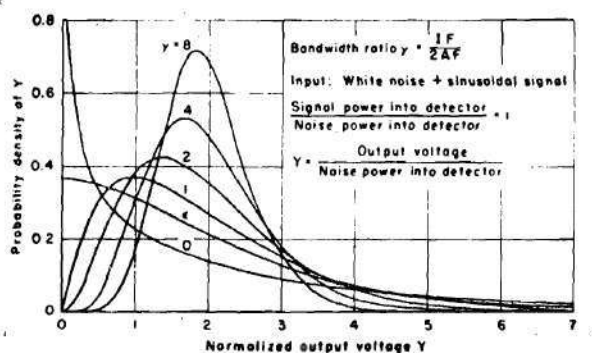


Figure 3. Output Probability Densities for the Emerson All-Gaussian System (Signal-to-Noise Ratio = 1).

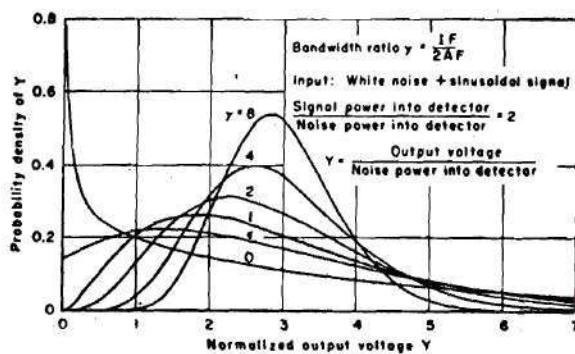


Figure 4. Output Probability Densities for the Emerson All-Gaussian System (Signal-to-Noise Ratio = 2).

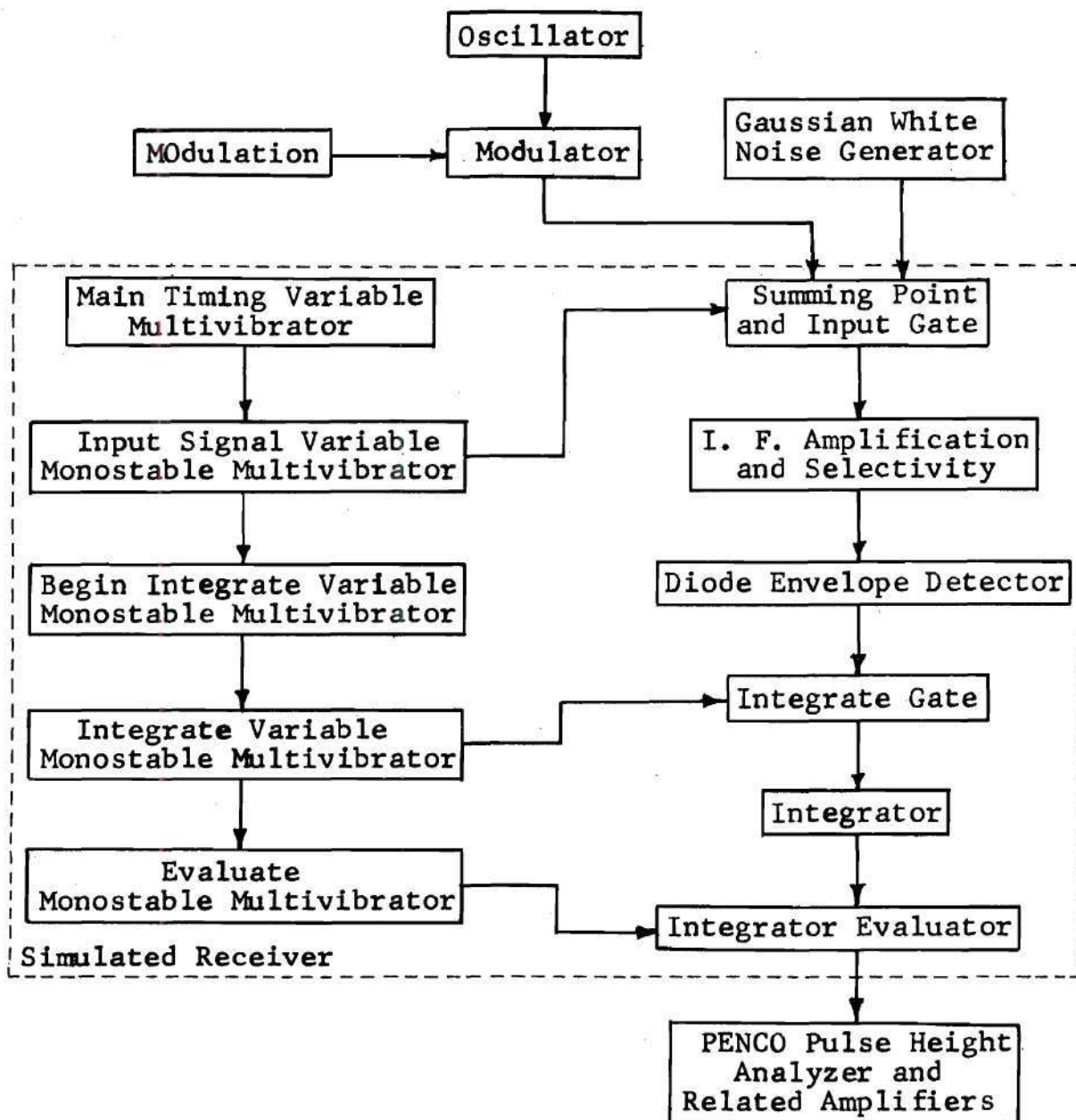


Figure 5. Block Diagram of the Simulated Receiver and Auxiliary Equipment.

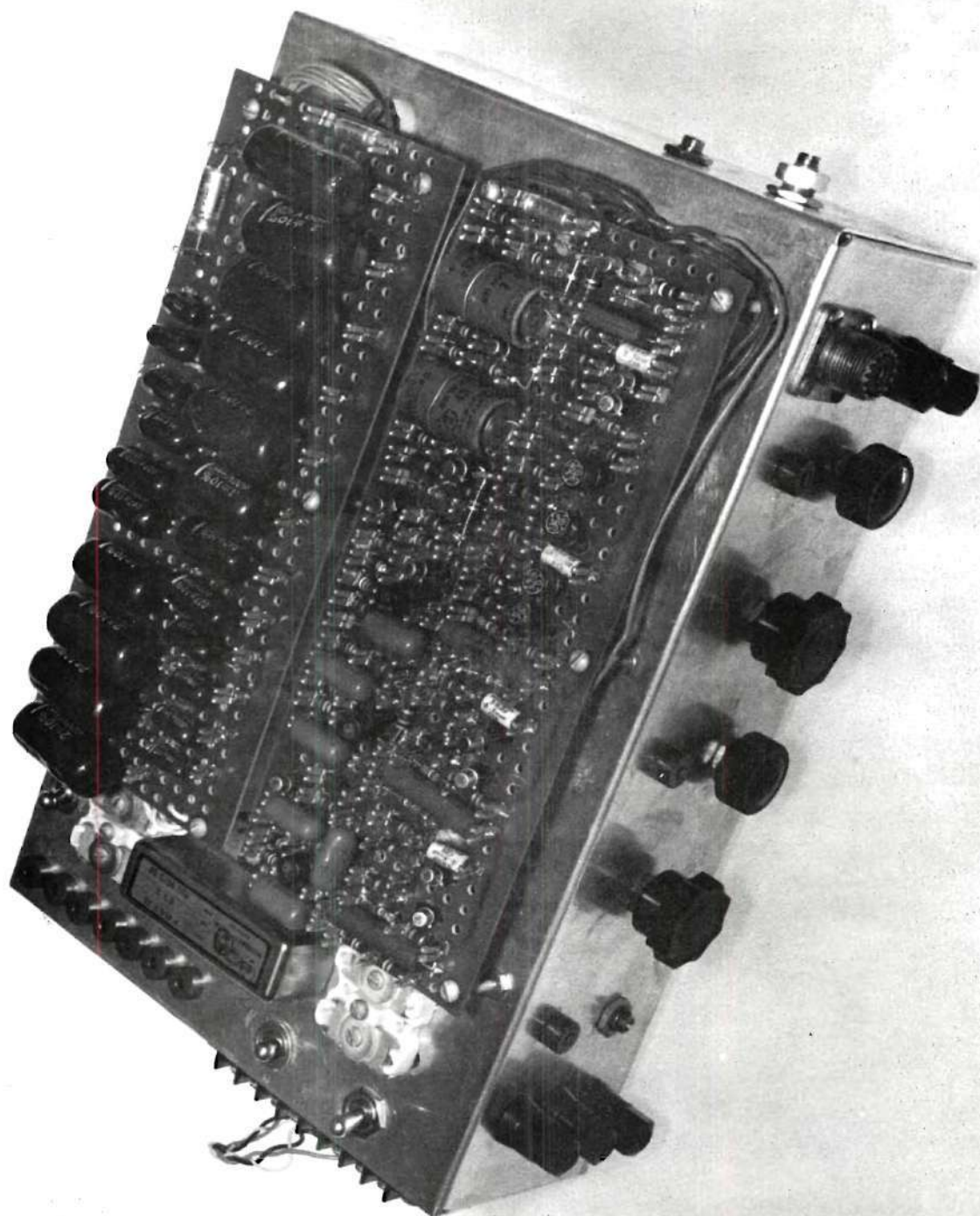
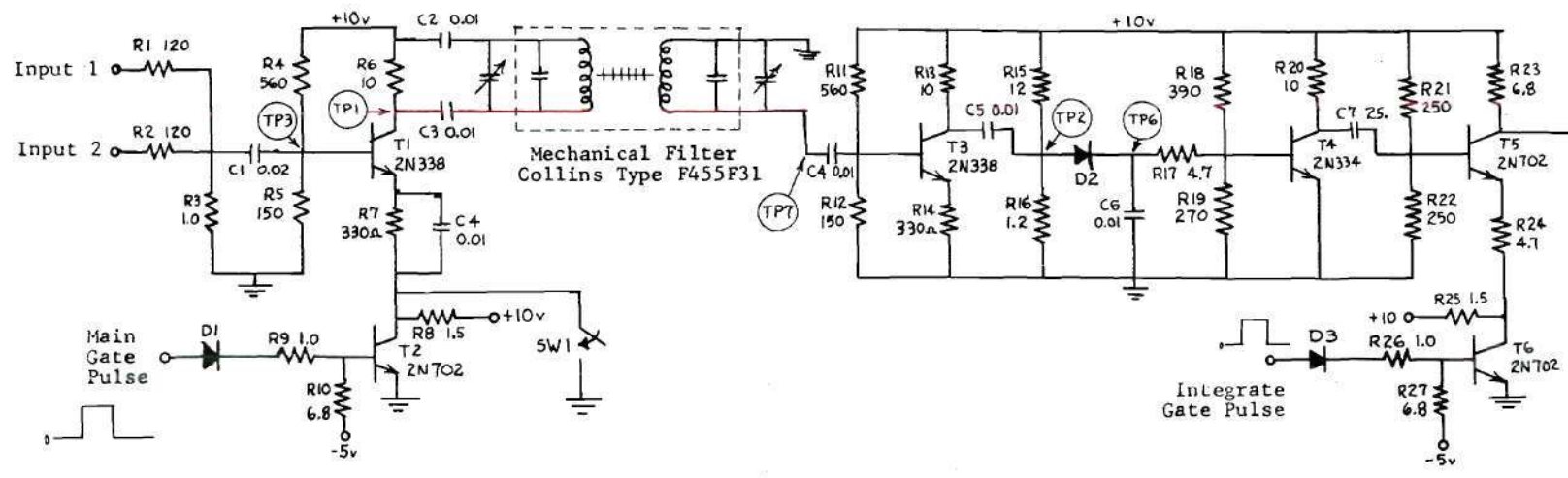


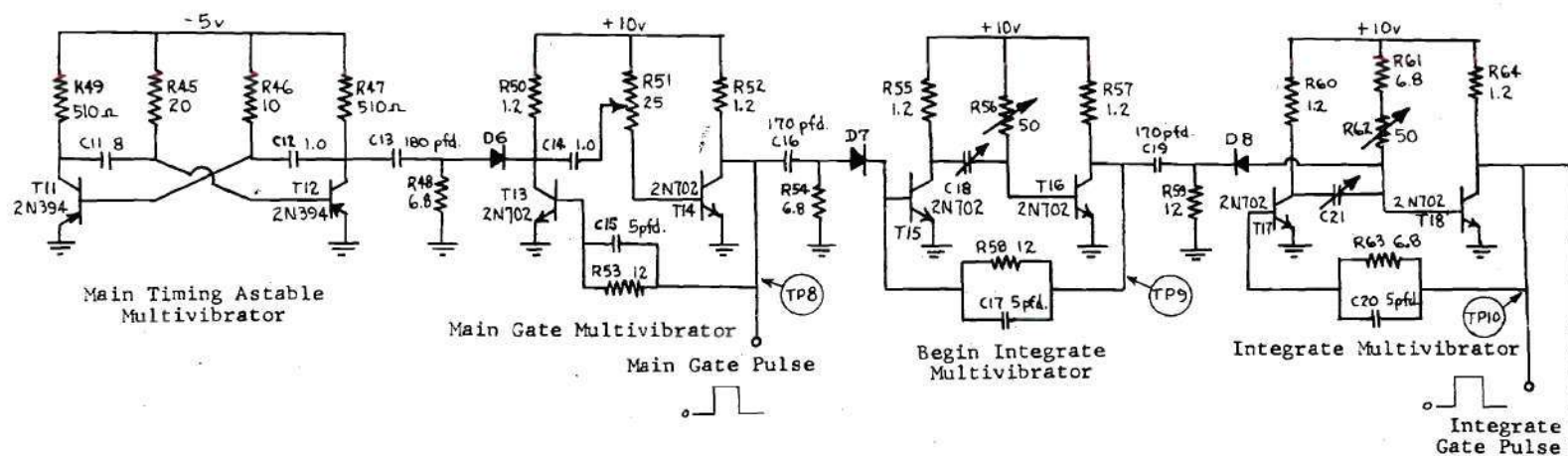
Figure 6. Photograph of the Simulated Receiver.



Notes:

1. All capacitances are in microfarads and resistances are in kilohms unless otherwise indicated. All diodes are 1N97.
2. C1 is chosen from among 0.047, 0.10, 0.20, 0.40, 1.0, 2.0, 4.0, and 6.0 microfarads by a front panel rotary switch.
3. Test points shown (TP *) are brought out to chassis jacks.
4. SW 1 overrides the Main Gate to allow continuous operation. SW 2 allows TP 5 to show the signal both before and after integration.

Figure 7. Schematic Diagram of the Simulated Receiver Excluding Timing Circuitry.



Notes:

1. All capacitances are in microfarads and all resistances are in kilohms unless otherwise shown. All diodes are 1N97.
2. Capacitors C18 and C21 are each selected from among 0.002, 0.0033, 0.0068, 0.012, 0.027, 0.047, 0.1, 0.2, and 0.4 microfarads by separate front panel rotary switches. The C2 rotary switch is in tandem with the C1 rotary switch described in the preceding figure.
3. Test points shown (TP *) are brought out to chassis jacks.

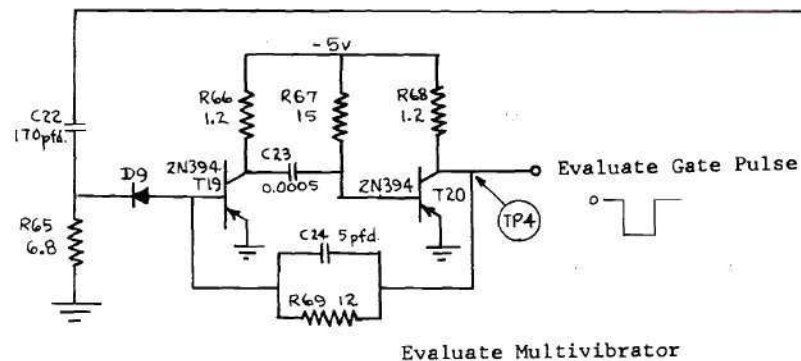


Figure 8. Schematic Diagram of the Simulated Receiver Timing Circuitry.

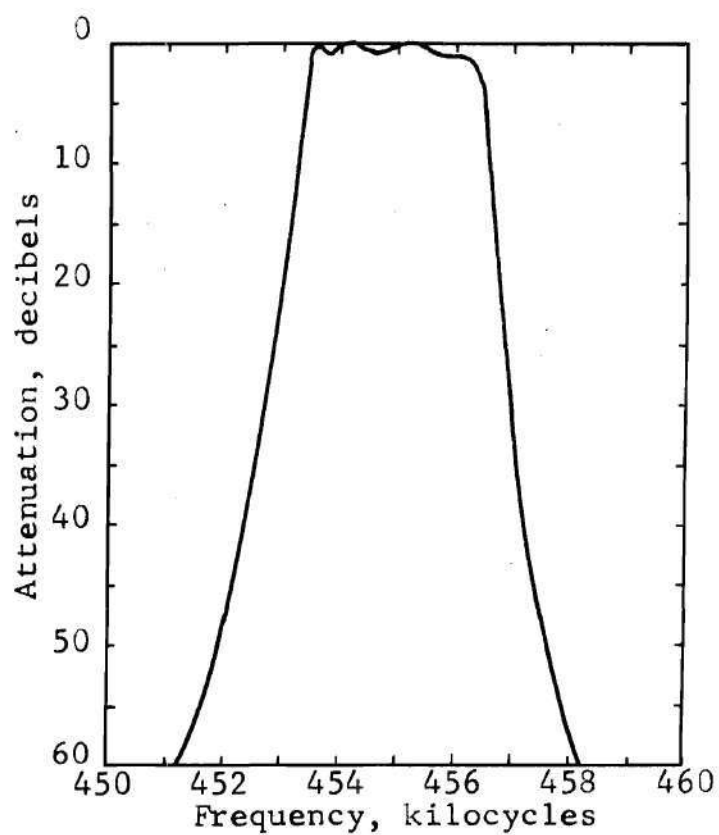
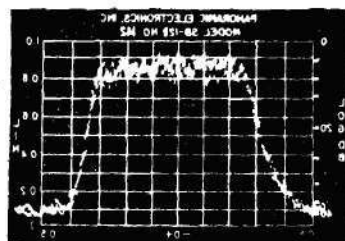


Figure 9. A Typical Mechanical Filter Selectivity Characteristic.



V: Log db H: 500 cps/division
(Note frequency increases to the left.)

Figure 11. Measured IF Selectivity of the Simulated Receiver.

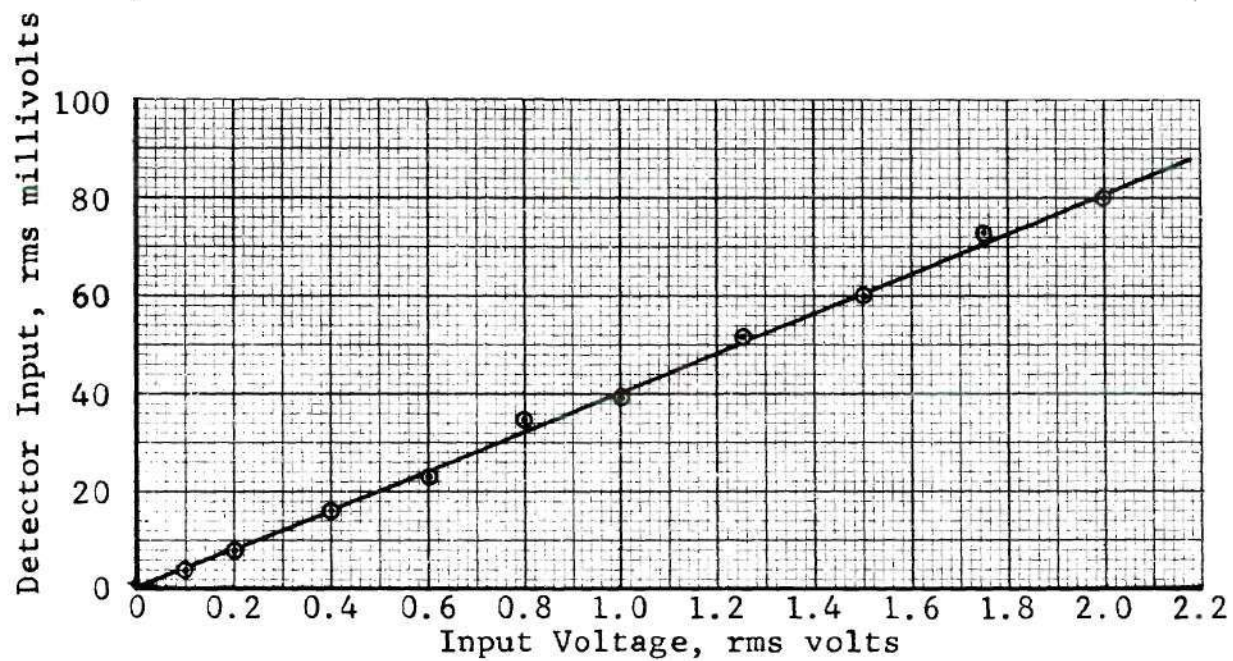


Figure 12. Linearity Test from the Equipment Input through the Detector Input.

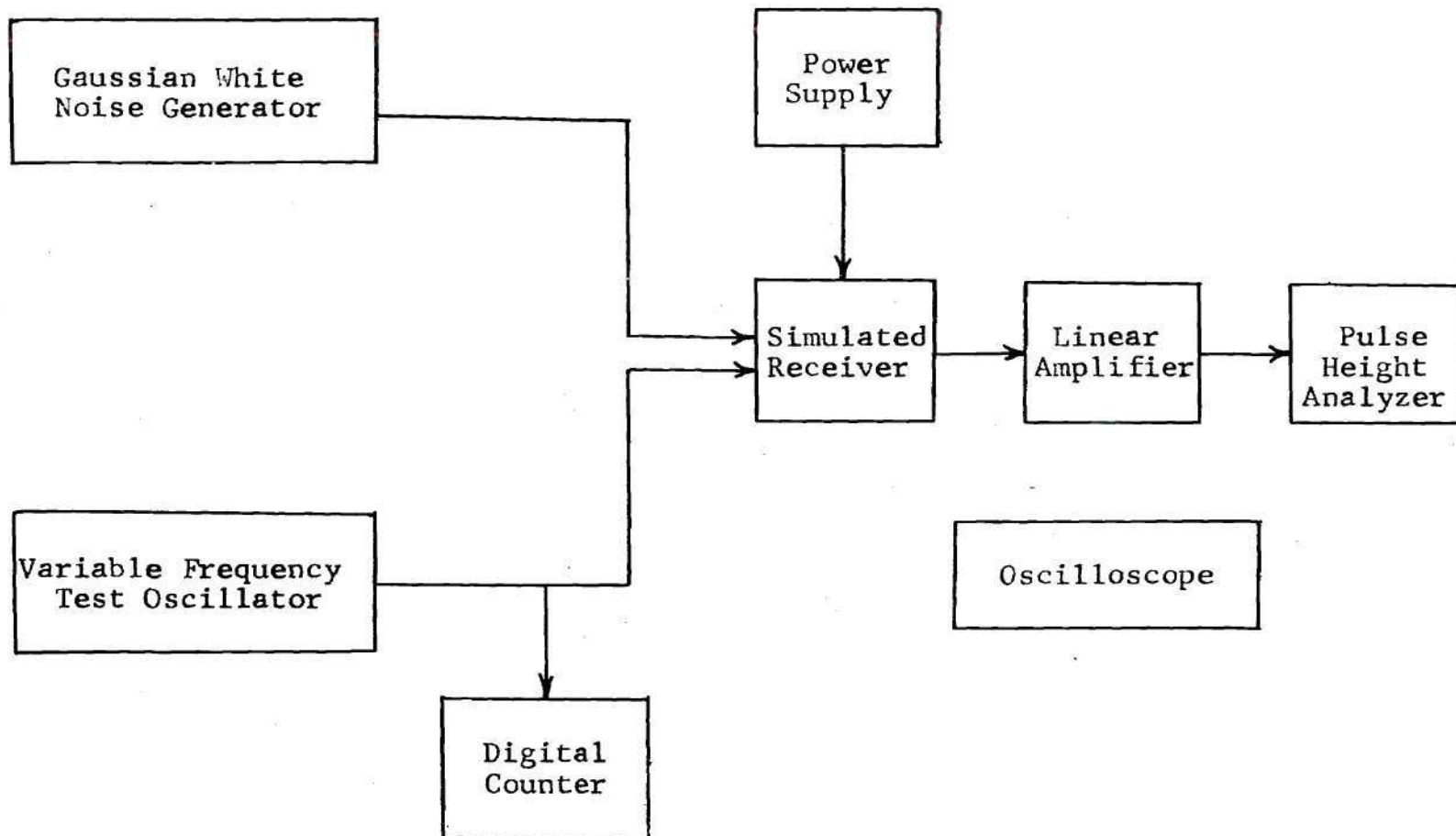


Figure 13. Operational Configuration for Simulated Receiver.

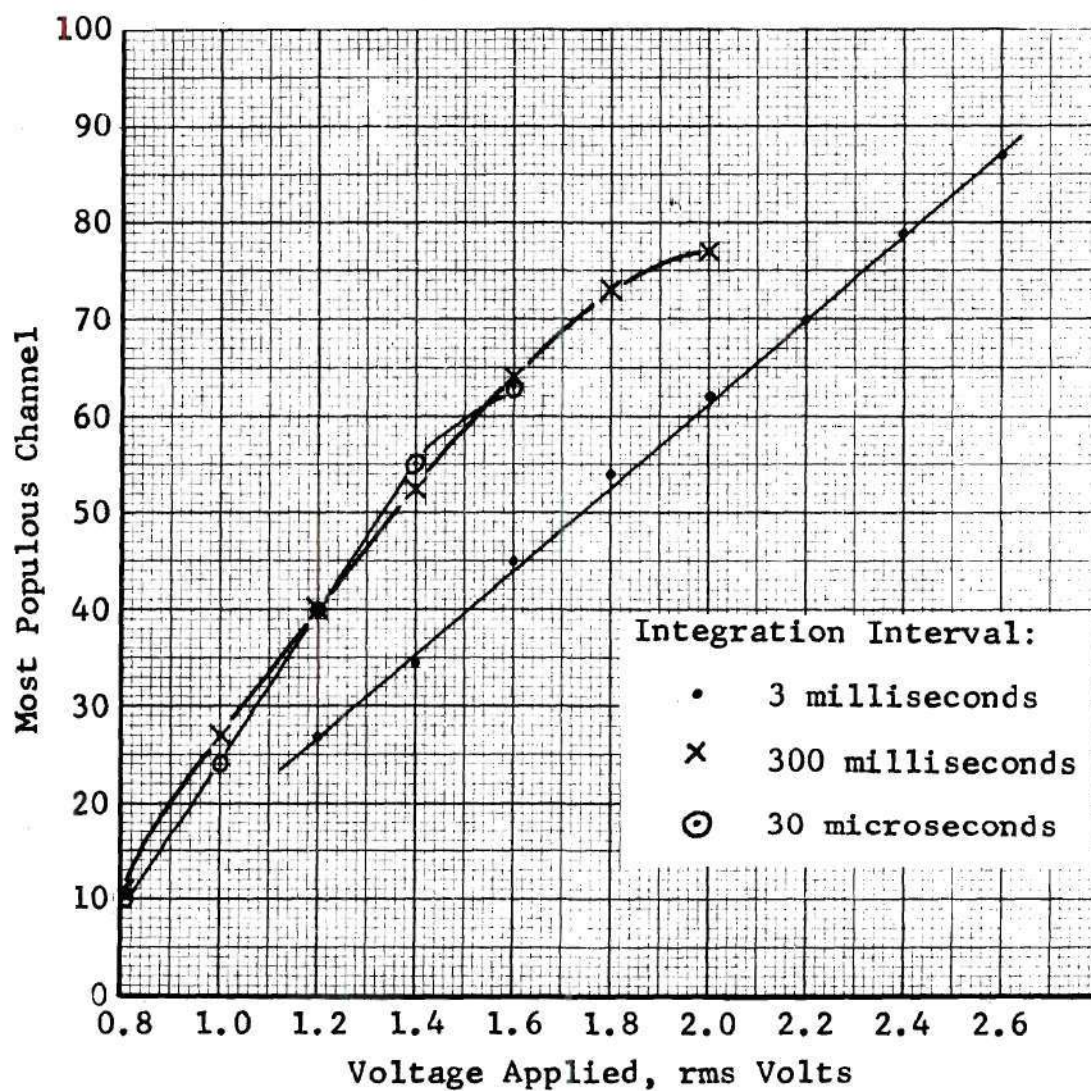


Figure 14. Investigation of System Linearity.

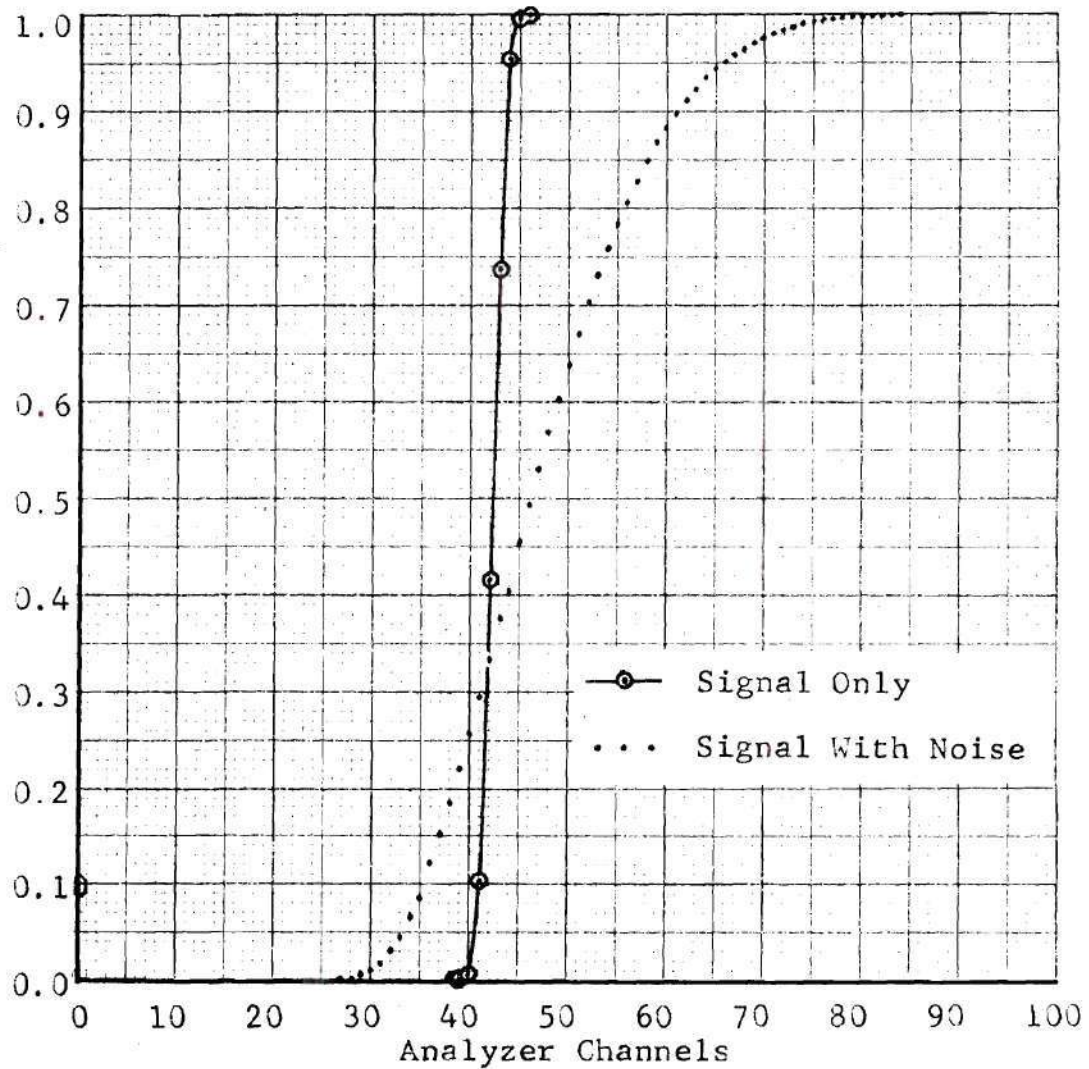


Figure 15. Output Probability Distribution Functions for a 100 Microsecond Integration Interval and $A_c/\sigma = 10$ db.

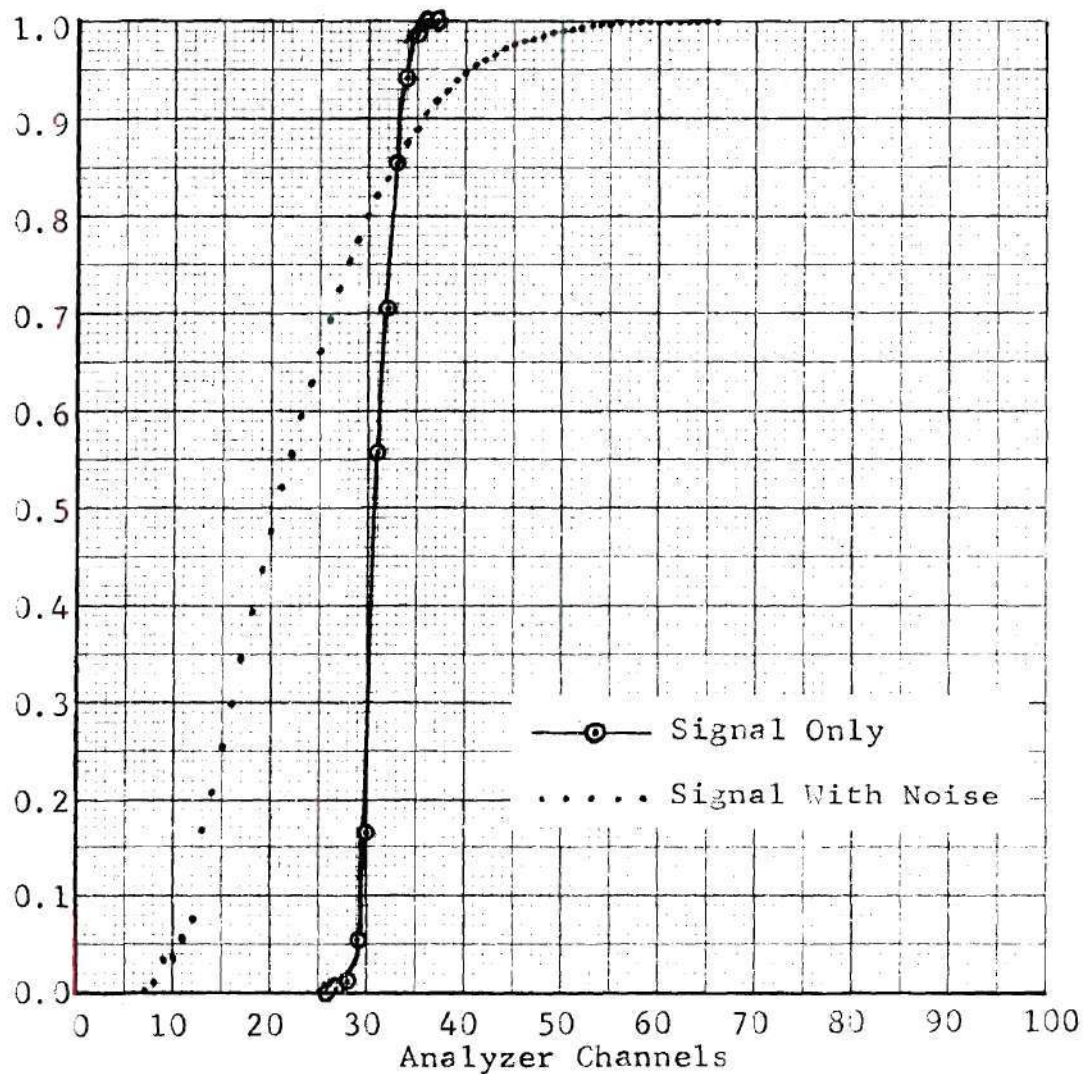


Figure 16. Output Probability Distribution Functions for a 300 Microsecond Integration Interval and $A_c/\sigma = 10$ db.

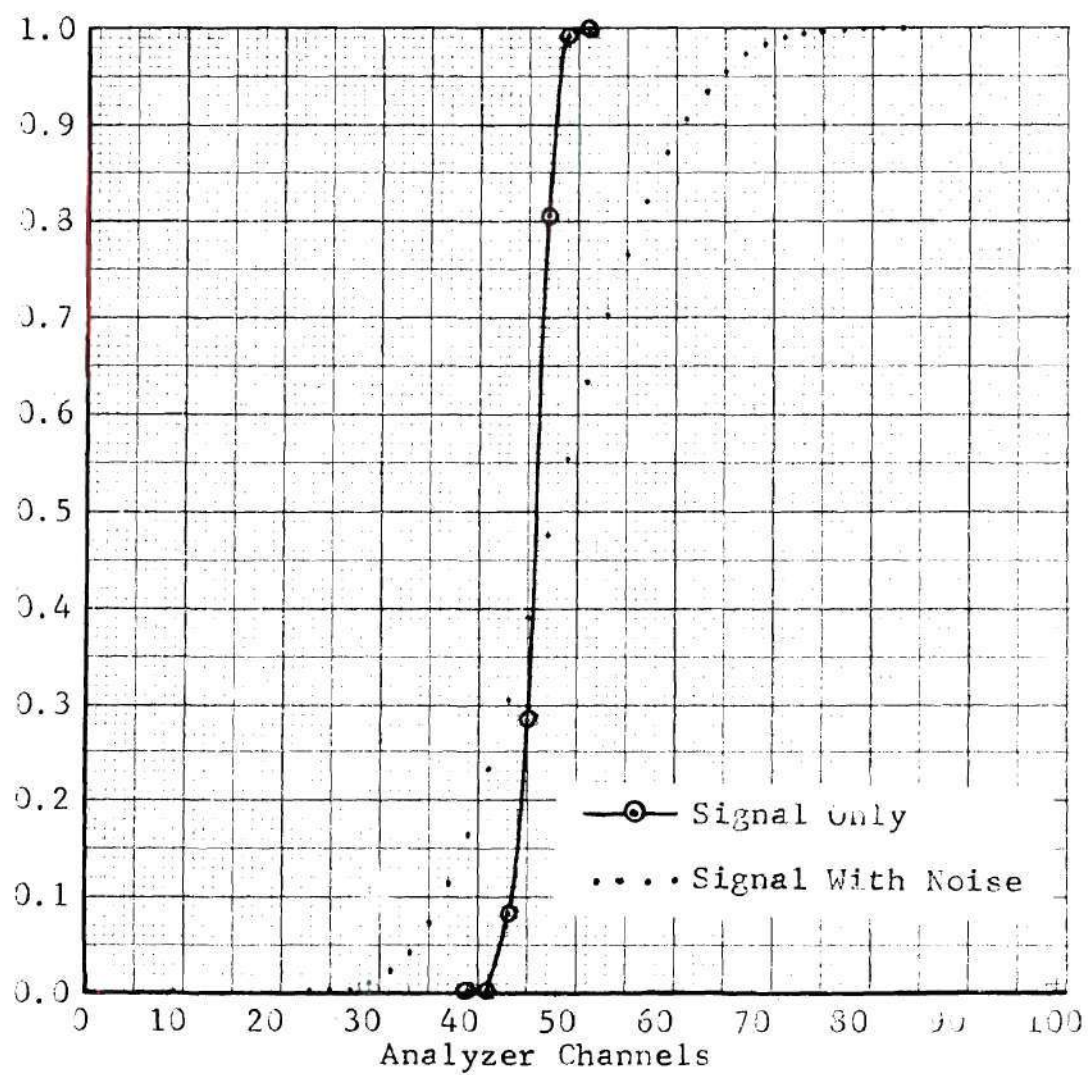


Figure 17. Output Probability Distribution Functions for a 1.0 Millisecond Integration Interval and $A_c/\sigma = 10$ db.

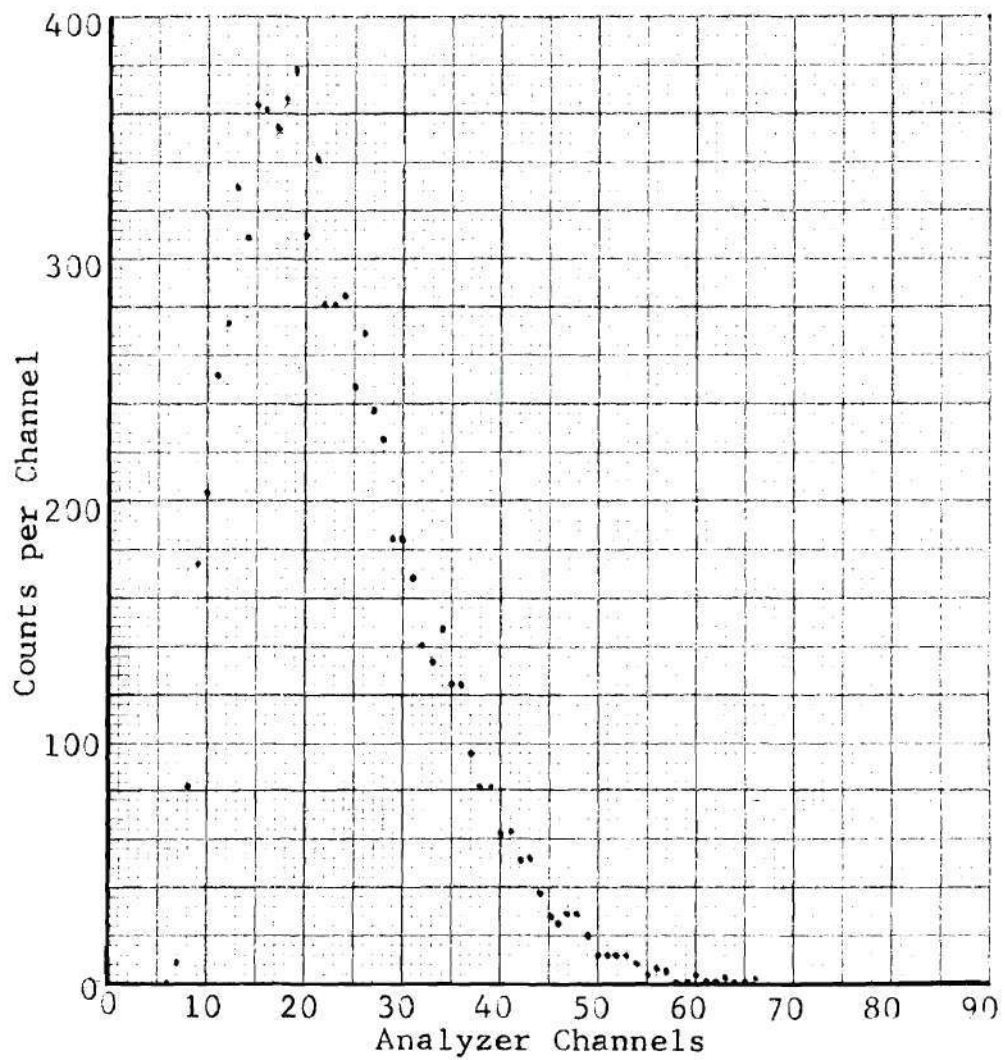


Figure 18. Output Probability Density Function for a 300 Microsecond Integration Interval and $A_c/\sigma = 10$ db.

A P P E N D I X

APPENDIX I

EQUIPMENT MANUAL

General Operating Procedure

The simulated receiver is designed to operate in the operational configuration shown in Figure A1. Power supply voltages required are +10 volts (yellow wire) and -5 volts (gray wire). The oscillator should be set for 455.0 kc and monitored (preferably with a digital counter) as the scales on most variable frequency oscillators are not sufficiently accurate. Figure A2 contains a layout diagram of the equipment with all inputs, controls, and outputs appropriately designated. An index of controls and their functions is contained in Figures A3(a) and A3(b). Figure A4(a through n) contains a summary of the test points and a typical waveform at each.

The following procedure should be followed in operating the equipment:

- (1) Connect the power supply to the equipment terminal strip +10 volts to the yellow wire, -5 volts to the gray wire and ground to the black wire.
- (2) Turn the equipment ON with the ON-OFF switch by switching it toward the rear of the equipment.
- (3) With the oscilloscope set for automatic triggering, place the test probe in the TP 8 test point receptacle and adjust the Main Gate potentiometer for the desired interval.

(4) Switch the oscilloscope to triggered operation and trigger from the TP 8 socket.

(5) Place the test probe in TP 9, vary the Begin Integrate rotary switch and the Begin Integrate potentiometer for the desired interval.

(6) Insert test probe in TP 10 and adjust the Integrate interval for the desired duration with the Integrate rotary switch and potentiometer.

(7) A check of the Evaluate gate signal can be made if desired on TP 4.

(8) The oscillator should be connected to either of the input terminals and adjusted for an output voltage of approximately 1.2 volts rms.

(9) Switch the Continuous Operation toggle switch toward the rear of the chassis for continuous operation and place the test probe in TP 7. Set the scope for maximum gain and a.c. operation. As the oscillator is tuned to 455.0 kc, the scope should indicate the presence of the carrier and the passband of the mechanical filter.

(10) Switch the Continuous Operation switch forward to gated operation. The TP 7 waveform should now indicate the ringing and delay characteristic of a pulsed signal passed through a narrowband filter. If an oscillator monitoring device is not available, 455 kc to sufficient accuracy is indicated by the sharpest rise time and an exponentially decaying ringing on the waveform.

(11) Disconnect the oscillator from the equipment and place the test probe with medium a.c. gain in TP 11. Make certain the Continuous Operation switch is forward and the equipment is, therefore, in the gated

mode of operation. The Integrate toggle switch should be to the left, or closed, so that signal will be applied to the integrator. Adjust the Well Balance potentiometer so that the well effect is exactly cancelled at the highest scope gain setting (5 millivolts per centimeter).

(12) With the signal still disconnected from the equipment place the test probe in either of the outputs. Adjust the oscilloscope for negative internal synchronization and expand the time scale to approximately 5 microseconds per centimeter. A pulse with approximately 2 microseconds rise time should be present, but in a slight "well." Adjust the Output potentiometer for maximum gain. CAREFULLY and LIGHTLY touch up the Well Balance potentiometer until the 1.5 microsecond flat portion of the output pulse is even with the base line or a very slight amount positive. Reconnection of the oscillator to the equipment should cause a positive shift in the pulse height. This is the signal-only or carrier-only output level.

(13) Noise may be connected to the equipment on the remaining input terminal. The measurement of the peak signal to rms noise ratio, A_c/σ , desired is made at TP 2, the detector input, with the equipment set for continuous operation by the Continuous Operation switch. After the A_c/σ ratio has been established, the equipment must be returned to gated operation.

(14) Operation of the pulse height analyzer will be outlined here insofar as the simulated receiver tests are concerned. No attempt should be made--nor would one be permitted--to operate the pulse height analyzer (PENCO) without instructions from those personnel responsible for the equipment. Connection to the auxiliary amplifiers should now

be made and the PENCO equipment placed in the operating mode.

(15) Gain of the auxiliary linear amplifier and the Output Potentiometer setting should be adjusted under all three simulator input conditions so that the desired spread is obtained in the data being compiled. It may be necessary to use only half of the analyzer's dynamic range, but with 0.5 volt channel widths.

(16) After appropriate gain settings have been determined, the PENCO equipment should be calibrated by applying varying amplitudes of signal-only input, including zero signal, into the simulator. Each input amplitude should be allowed to run for approximately three to five minutes. This calibration data should then be printed out for later use.

(17) The desired A_c/σ test can now be run. Accumulate data only until a sufficiency has been obtained, which should occur in approximately ten minutes of running time. Print the data.

(18) Disconnect the noise generator and make a run with signal only of approximately three minutes and a no-signal run of the same length to assure that the equipment has not drifted during the just completed signal-to-noise data run.

Equipment Layout

In addition to the general layout diagram of Figure A2, Figure A5, A6 and A7 present the component layout diagrams for the three phenolic circuit boards used. In order that the Equipment Manual will be independent of the body of the thesis, the circuit diagrams given as Figure 8 and 9 in the text are repeated identically here as Figures A9 and A10.

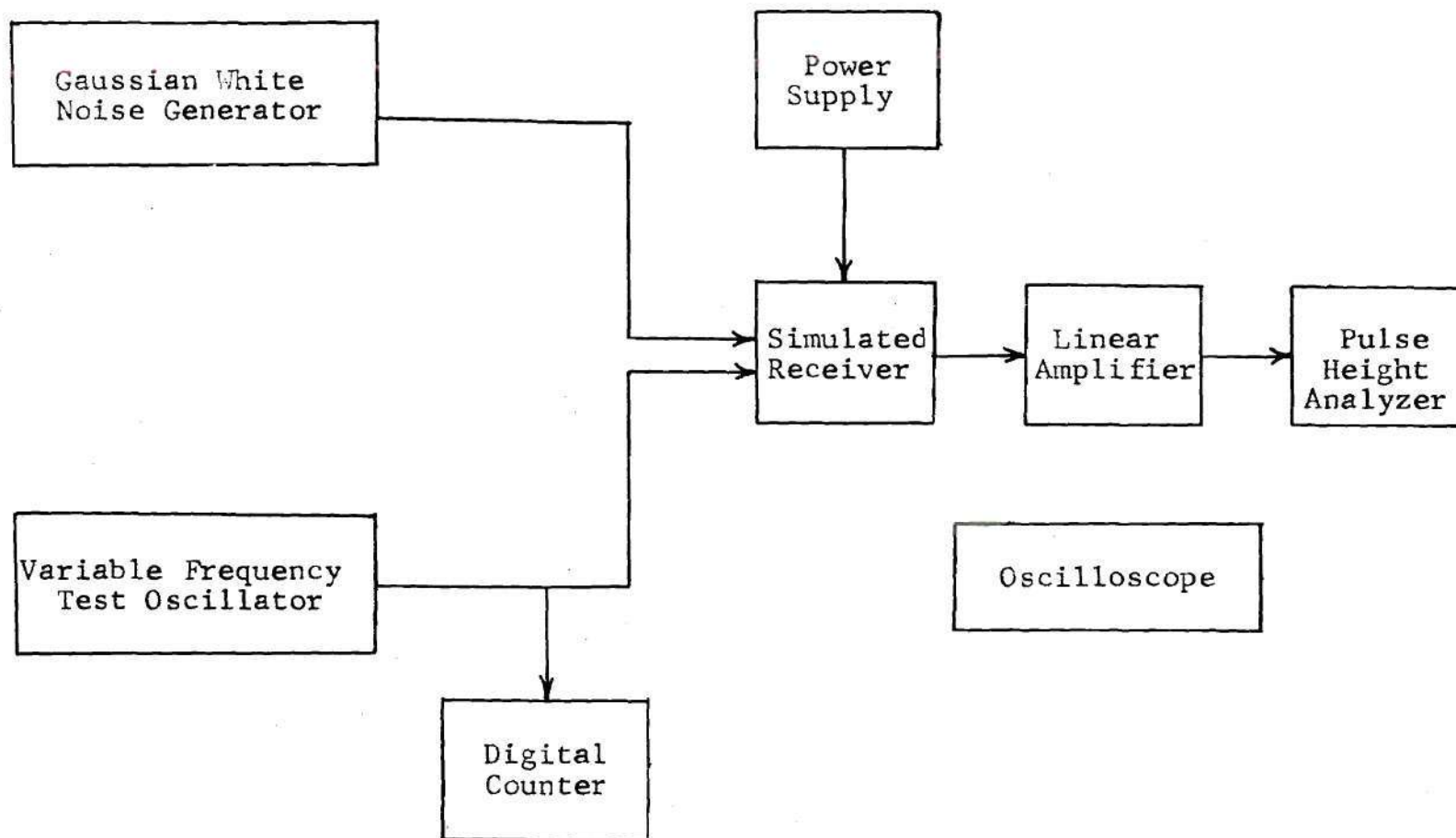


Figure A1. Operational Configuration for Simulated Receiver.

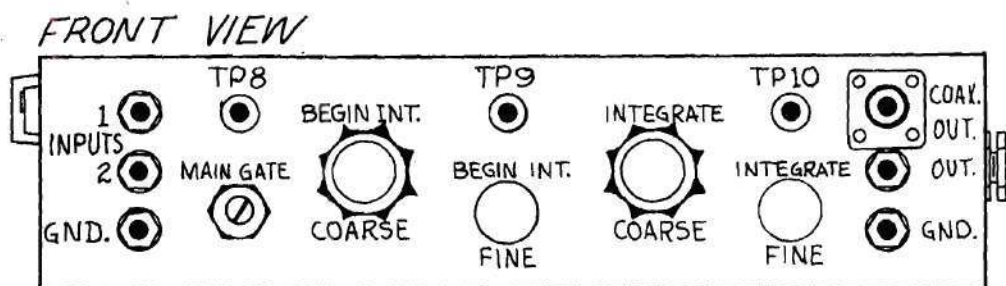
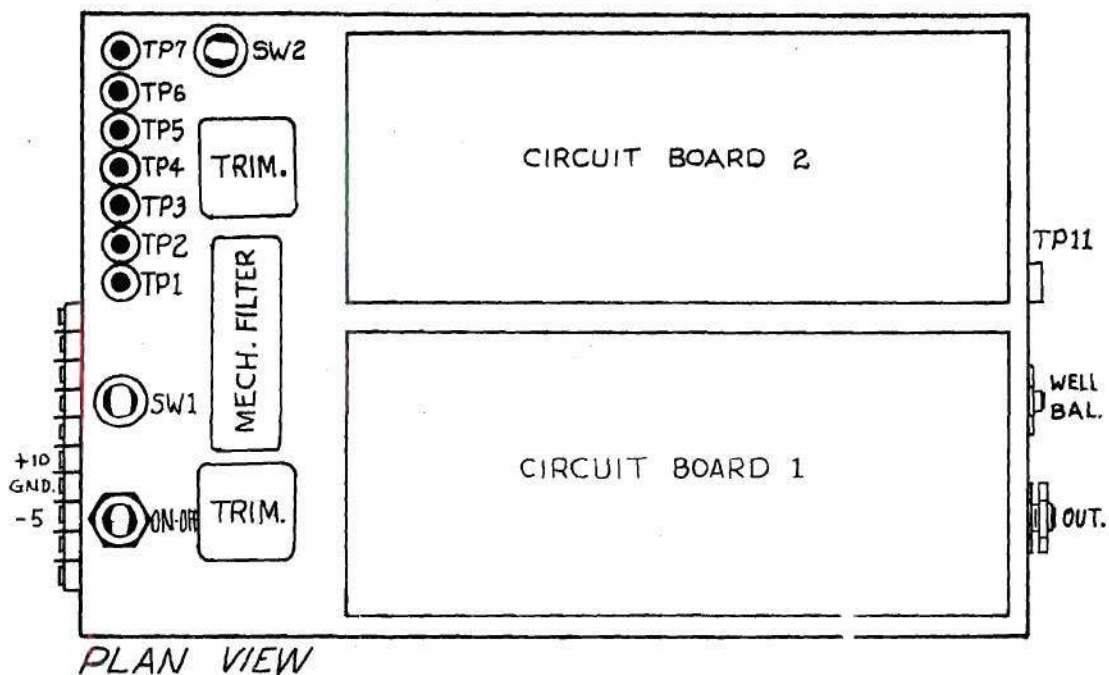


Figure A2. General Layout Diagram of the Simulated Receiver.

INDEX OF CONTROLS

CONTROL	LOCATION	FUNCTION
1. ON-OFF toggle switch	Left front top	Applies 10 volts and -5 volts bias to equipment circuits when toward rear.
2. Continuous Operation toggle switch	Left center top	Grounds emitter of T1 to defeat gating by T2 and thereby admitting signal continuously.
3. Integrate toggle switch	Left rear top	Applies signal to integrator when toward left and opens circuit ahead of integrator when toward right. Switches TP 5.
4. Main Gate potentiometer	Left front	Controls time constant of main gate multivibrator and thereby the duration of main signal gate, T2.
5. Begin Integrate rotary switch	Left-center front	Provides step control in factors of two of Begin Integrate multivibrator time constant. (Thereby controls start of integrate interval.)
6. Begin Integrate potentiometer	Center front	Provides fine control of Begin Integrate multivibrator time constant and, thereby, of the start of the integrate interval.
7. Integrate rotary switch	Right-center front	Provides step control in factors of two of Integrate multivibrator time constant. (Thereby controls duration of Integrate interval and start of Evaluate interval.)

Figure A3. An Index of the Location and Functions of the Various Switches and Other Equipment Controls. (Continued on next page.)

INDEX OF CONTROLS (CONTINUED)

- | | | |
|--------------------------------|-------------------|--|
| 8. Integrate potentiometer | Right front | Provides fine control of Integrate multi-vibrator time constant and, thereby, of the duration of the Integrate interval. |
| 9. Output potentiometer | Right side, front | Varies amplitude of output pulses. |
| 10. Well Balance potentiometer | Right side, rear | Provides control of the signal supplied to counteract the well effect just prior to the integrator. |

Figure A3. (Continued).

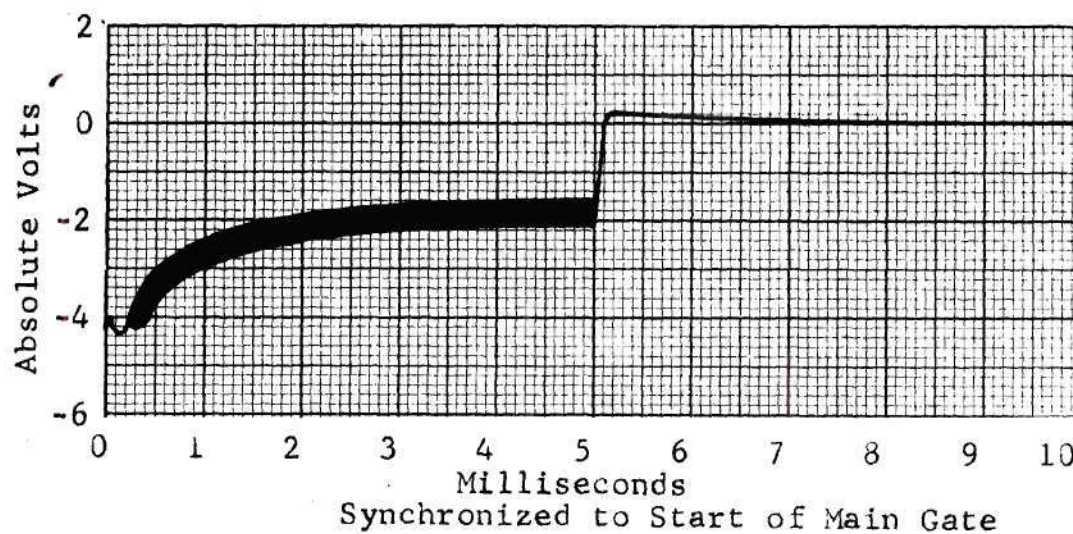


Figure A4(a). Waveform at TP 1 for a 5.0 Millisecond Main Gate Interval and a 1.20 Volt rms Input Signal.

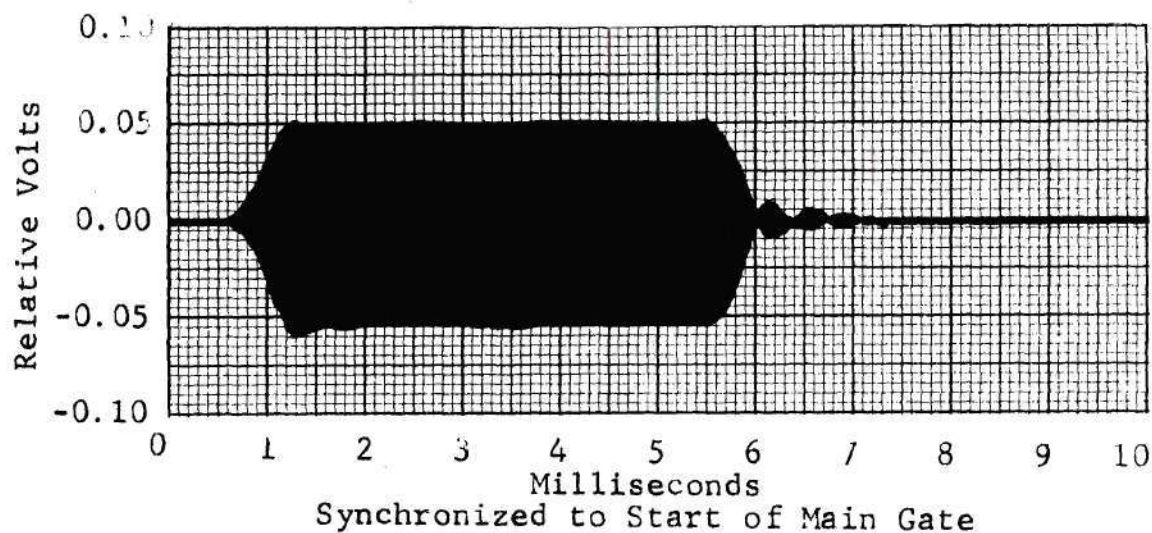


Figure A4(b). Waveform at TP 2 for a 5.0 Millisecond Main Gate Interval and a 1.20 volt rms Input Signal.

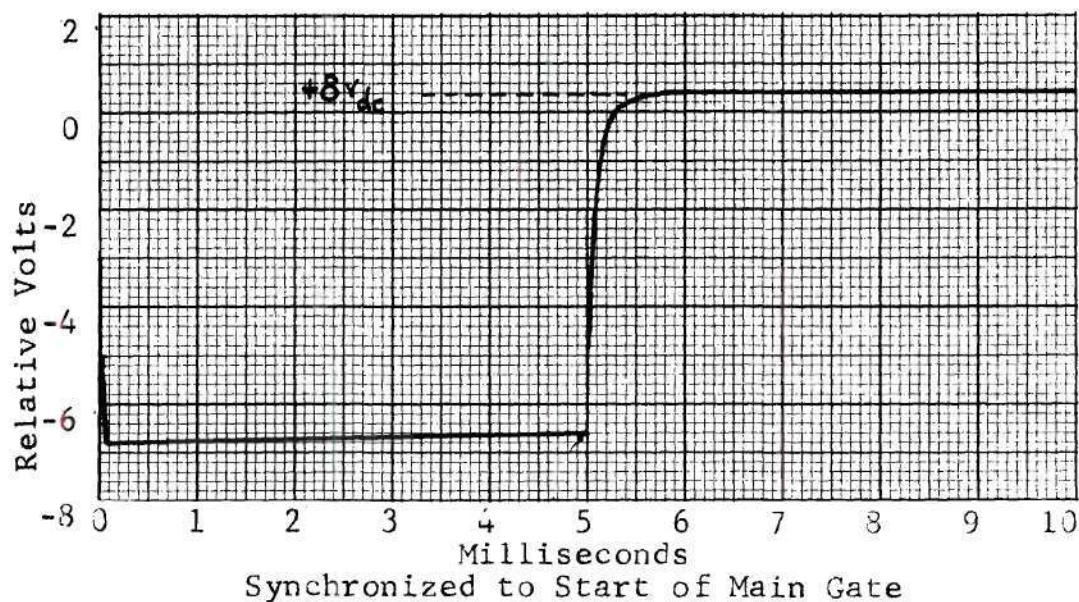


Figure A4(c). Waveform at TP 3 for a 5.0 Millisecond Main Gate Interval and a 1.20 Volt rms Input Signal.

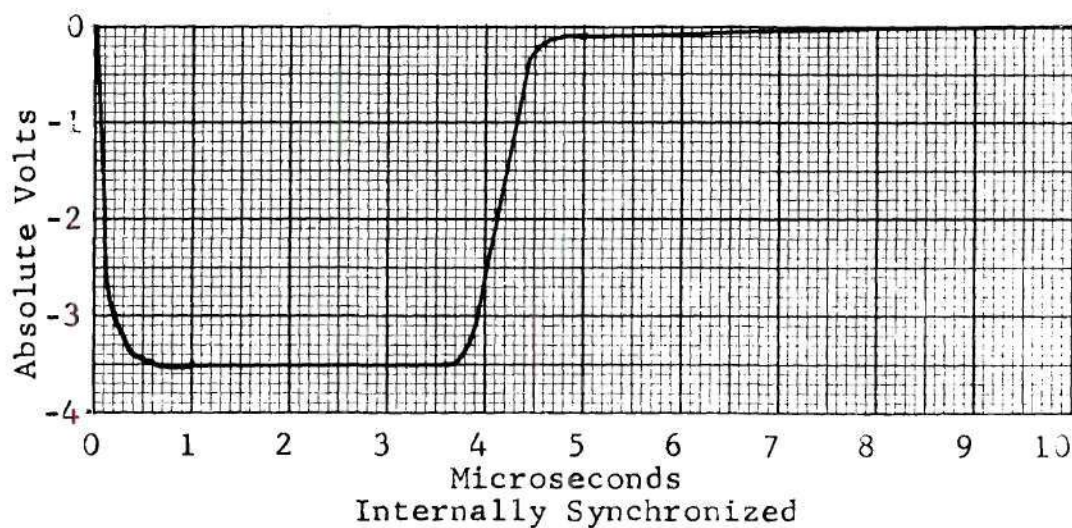


Figure A4(d). Waveform at TP 4.

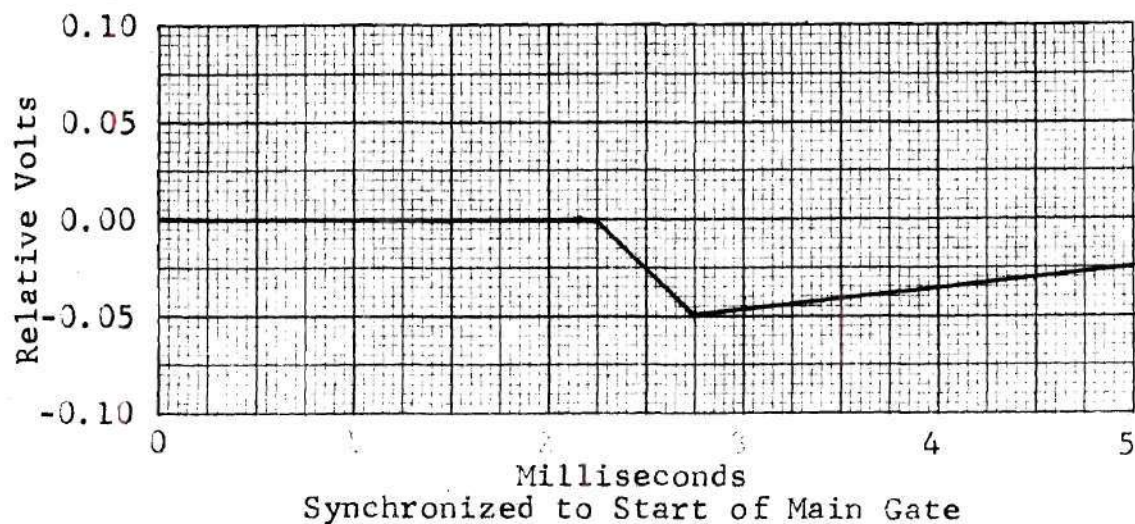


Figure A4(e). Waveform at TP 5 With SW 2 Closed for an Integration Interval of 0.5 Millisecond and a 1.20 Volt rms Input Signal.

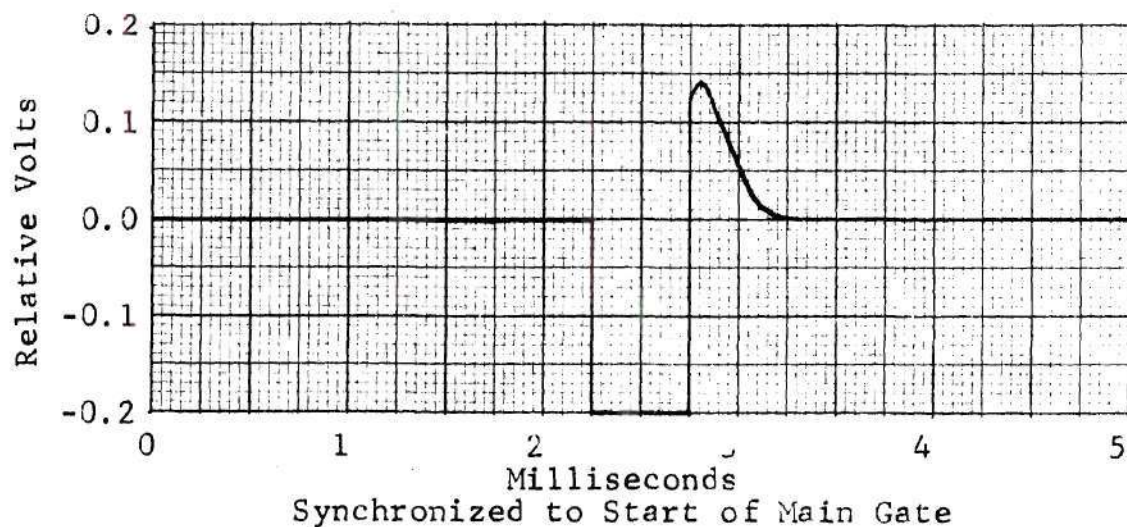


Figure A4(f). Waveform at TP 5 With SW 2 Open for an Integration Interval of 0.5 Millisecond and a 1.20 Volt rms Input Signal.

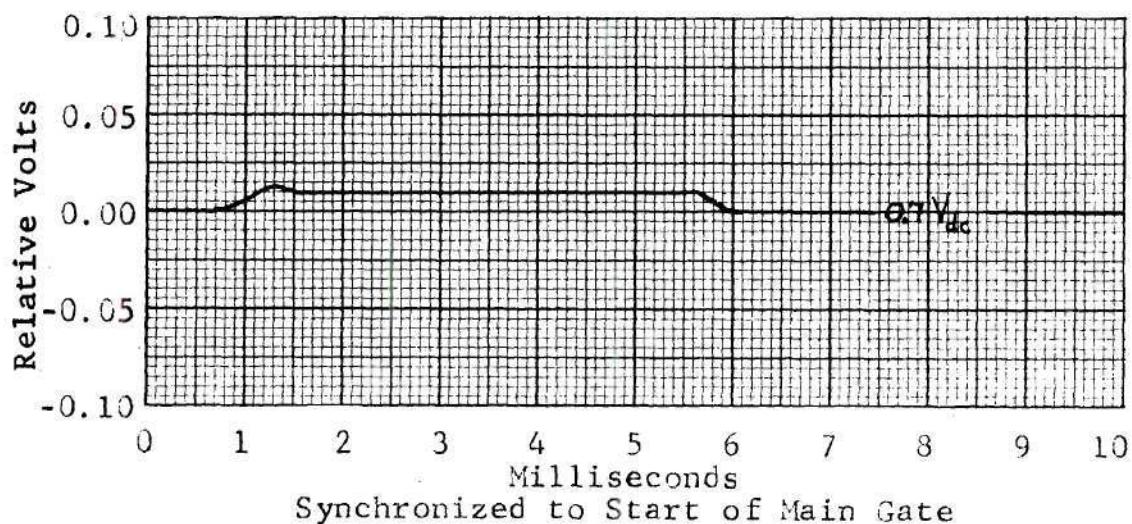


Figure A4(g). Waveform at TP 6 With a 5.0 Millisecond Main Gate Interval and an Input Signal of 1.20 Volts rms.

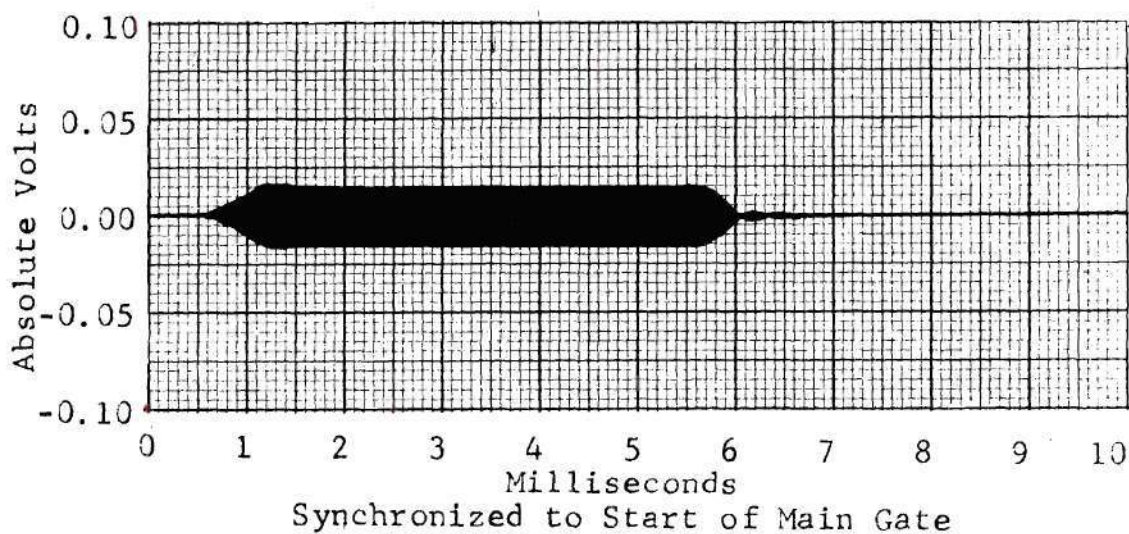


Figure A4(h). Waveform at TP 7 With a 5.0 Millisecond Main Gate Interval and an Input Signal of 1.20 volts rms.

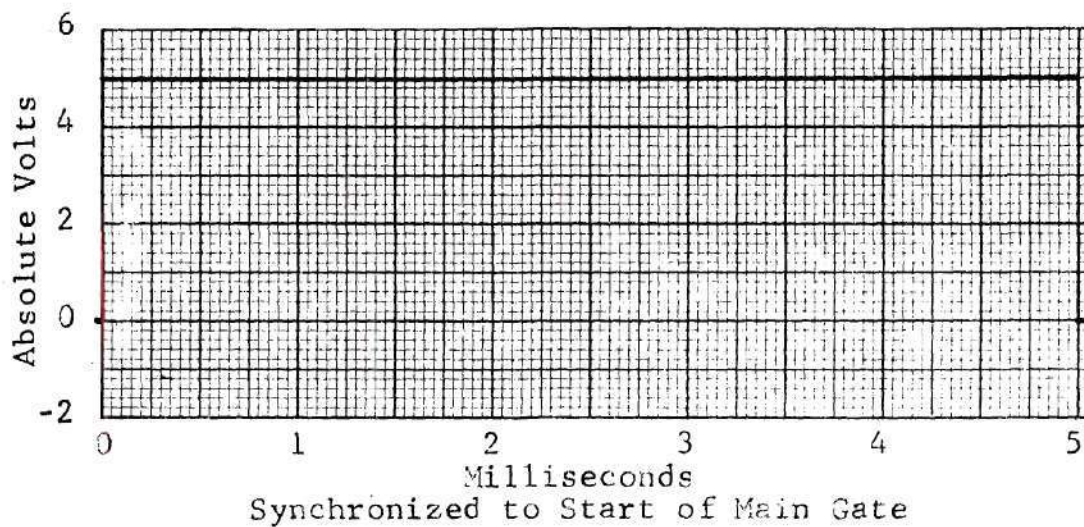


Figure A4(i). Waveform at TP 3 for a 5.0 Millisecond Main Gate Interval.

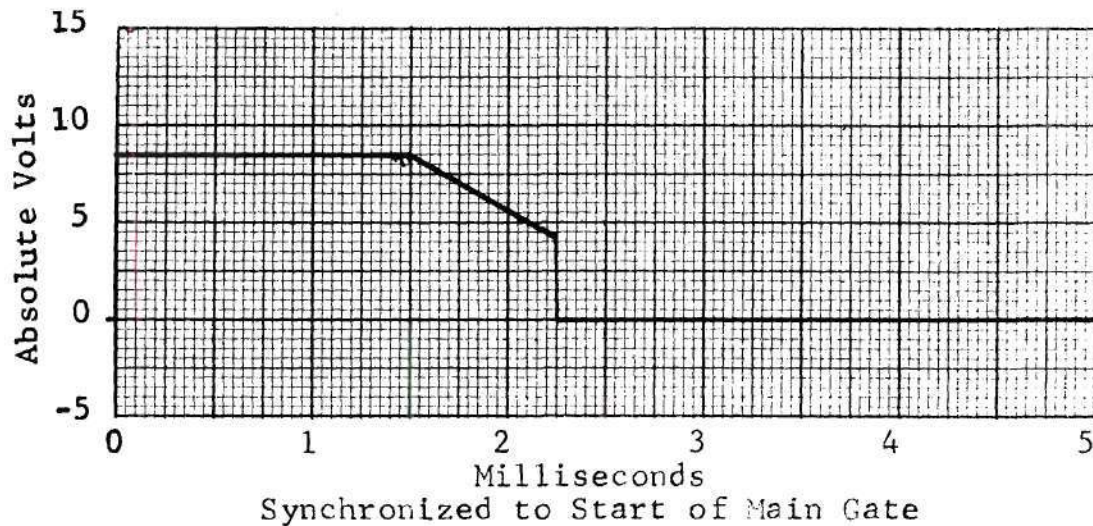


Figure A4(j). Waveform at TP 9 for a 2.25 Millisecond Begin Integrate Interval.

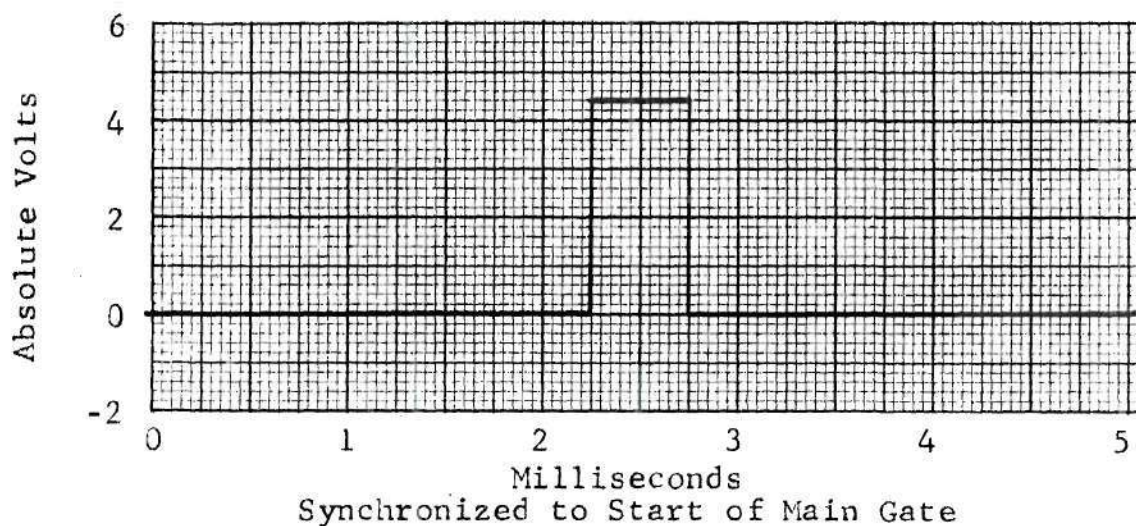


Figure A4(k). Waveform at TP 10 for a 0.5 Millisecond Integration Interval.

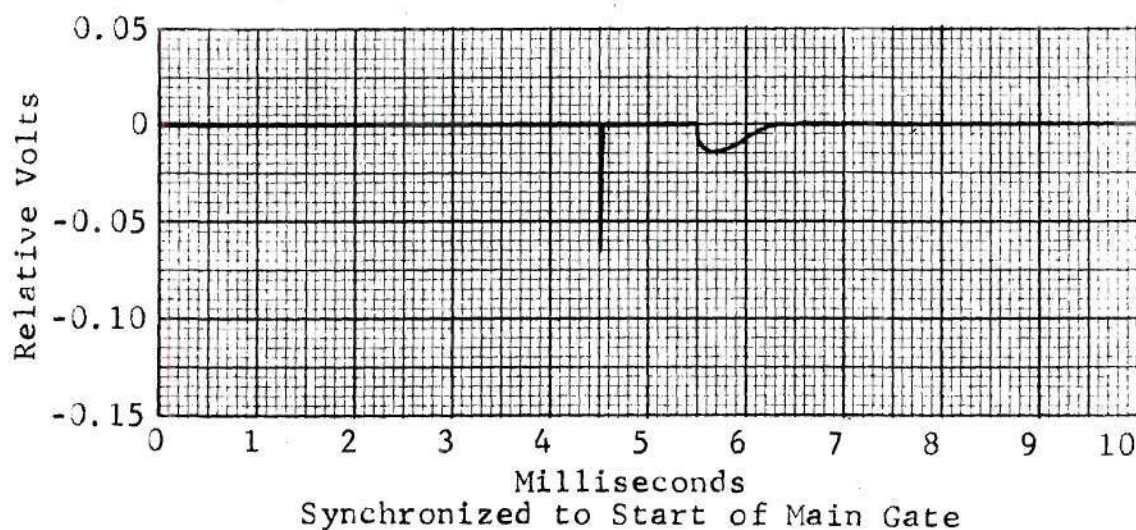


Figure A4(l). Waveform at TP 11 With No Input to the Simulated Receiver and An Integration Interval of 0.5 Millisecond. Note the Well Cancellation in the Integration Interval.

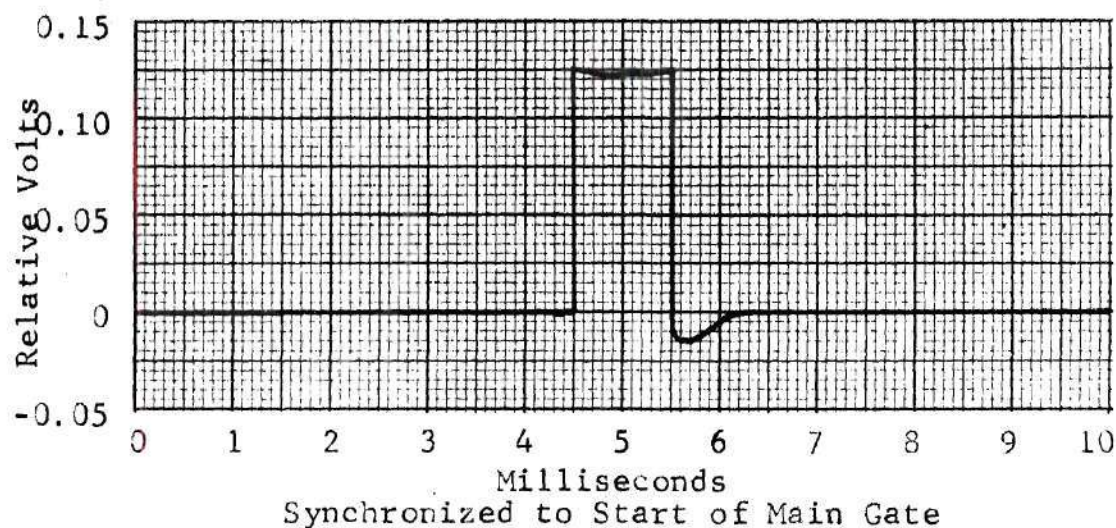


Figure A4(m). Waveform at TP 11 with an Input of 1.20 Volts rms and an Integration Interval of 0.5 Milliseconds.

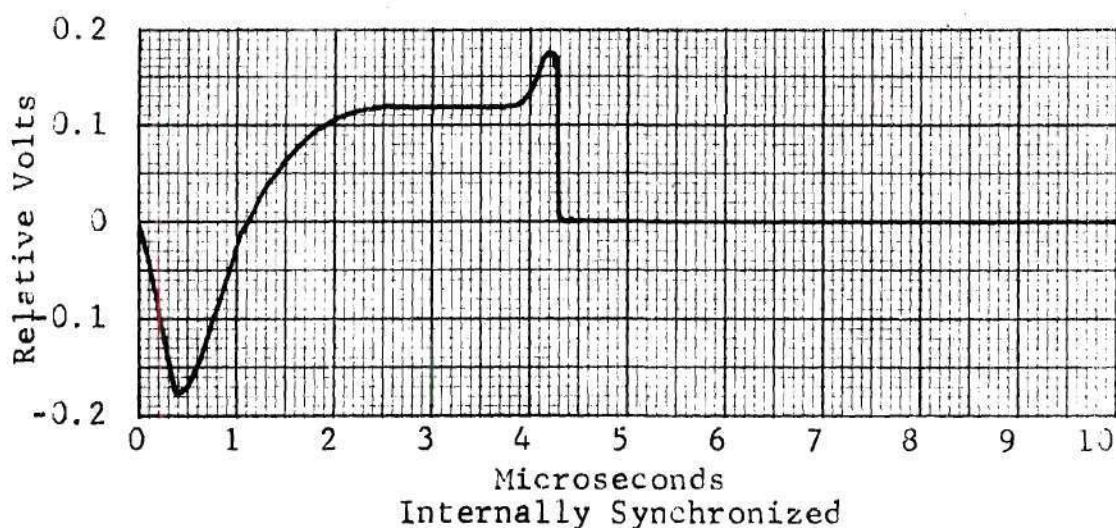


Figure A4(n). An Output Pulse Generated by the Simulated Receiver When Operated with a Main Gate Interval of 5.0 Milliseconds, an Integration Interval of 0.5 Milliseconds, and an Input Signal of 1.20 Volts rms.

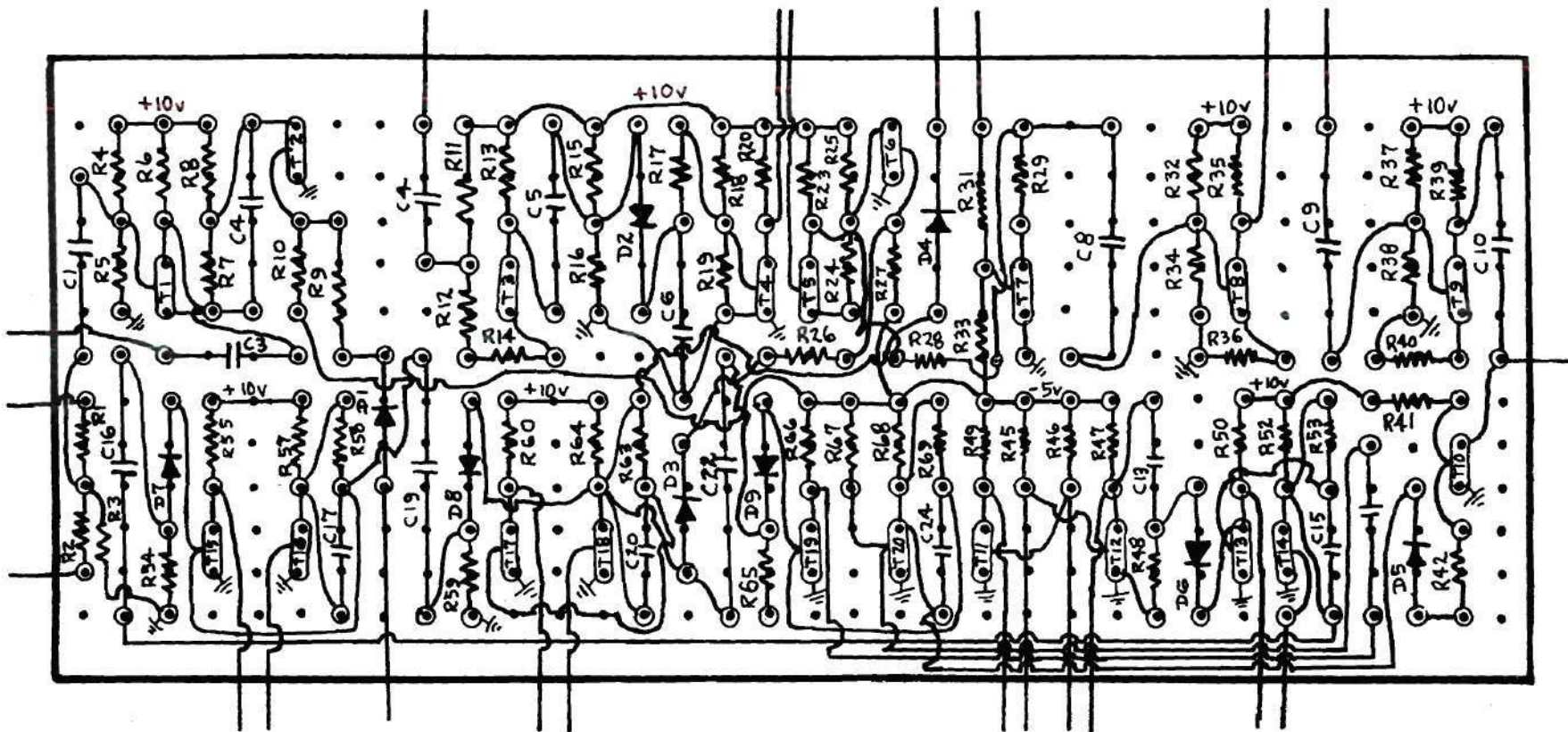


Figure A5. Component Layout Diagram, Circuit Board 1.

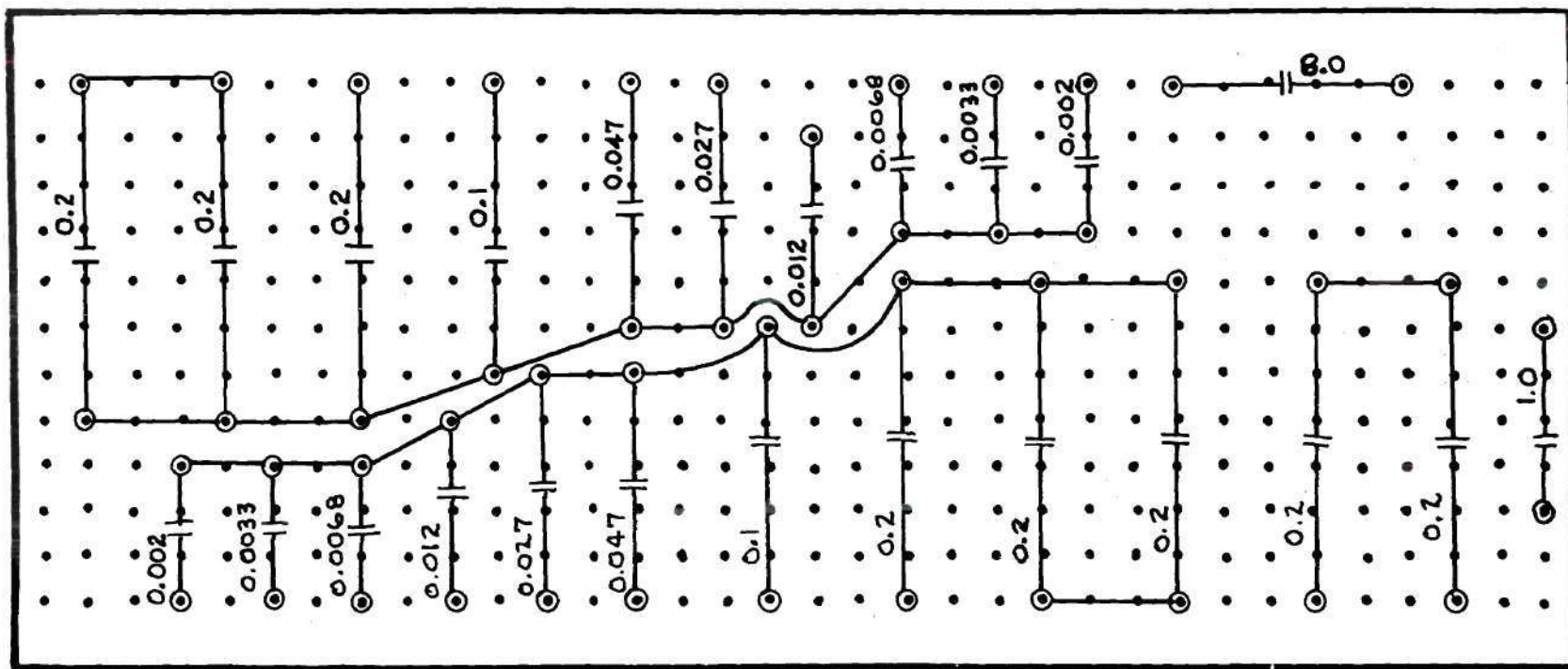


Figure A6. Component Layout Diagram, Circuit Board 2.

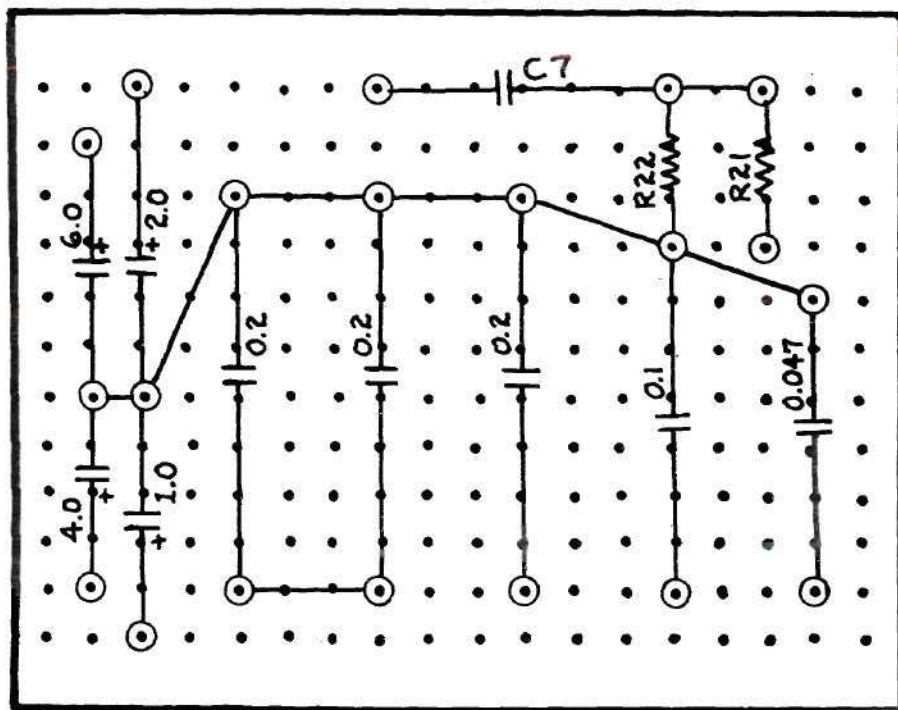
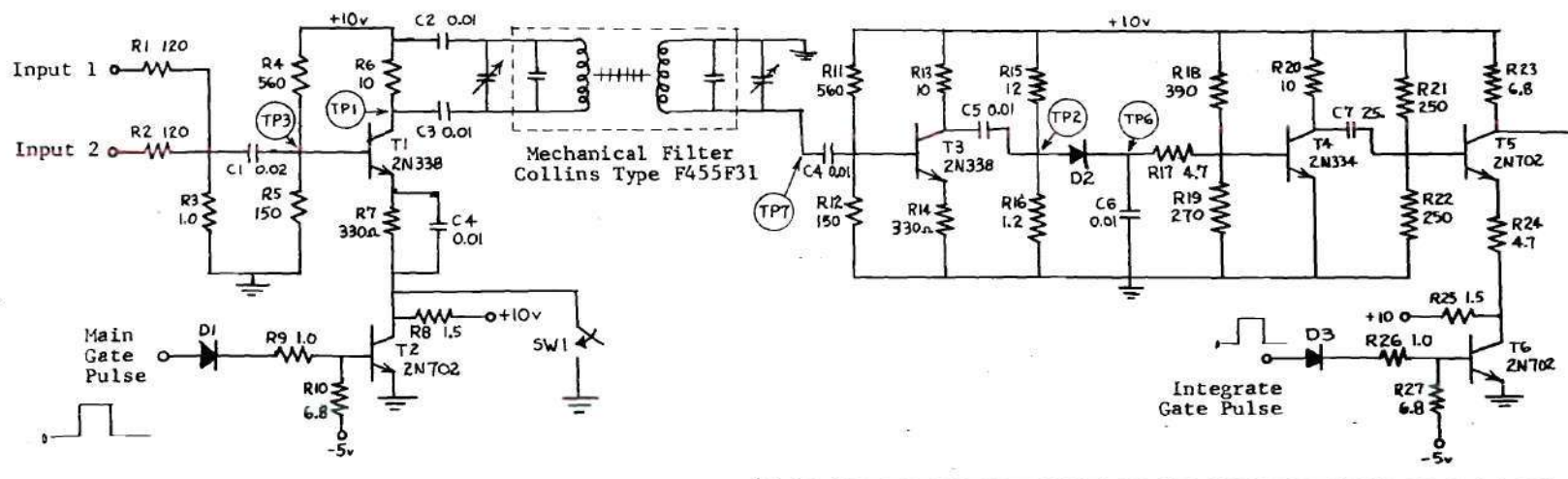


Figure A7. Component Layout Diagram, Circuit Board 3.



Notes:

1. All capacitances are in microfarads and resistances are in kilohms unless otherwise indicated. All diodes are 1N97.
2. CI is chosen from among 0.047, 0.10, 0.20, 0.40, 1.0, 2.0, 4.0, and 6.0 microfarads by a front panel rotary switch.
3. Test points shown (TP *) are brought out to chassis jacks.
4. SW 1 overrides the Main Gate to allow continuous operation. SW 2 allows TP 5 to show the signal both before and after integration.

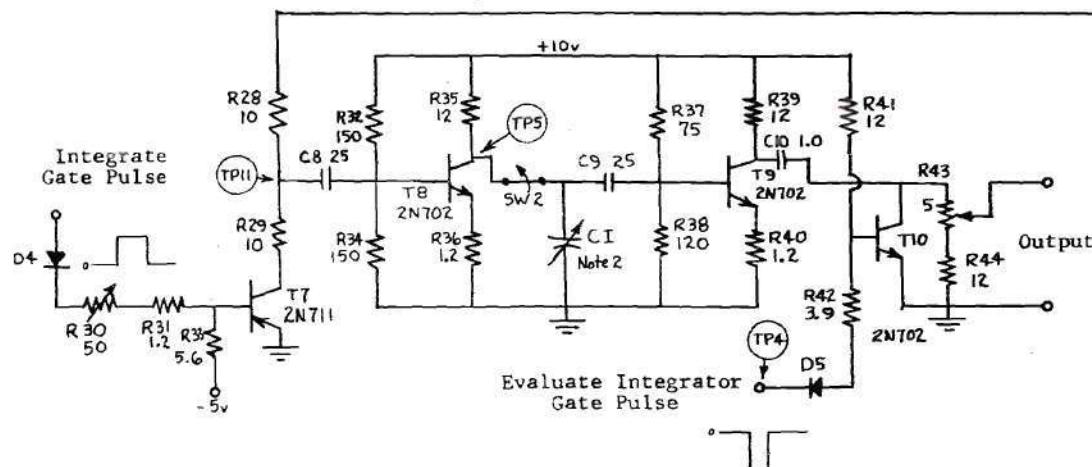
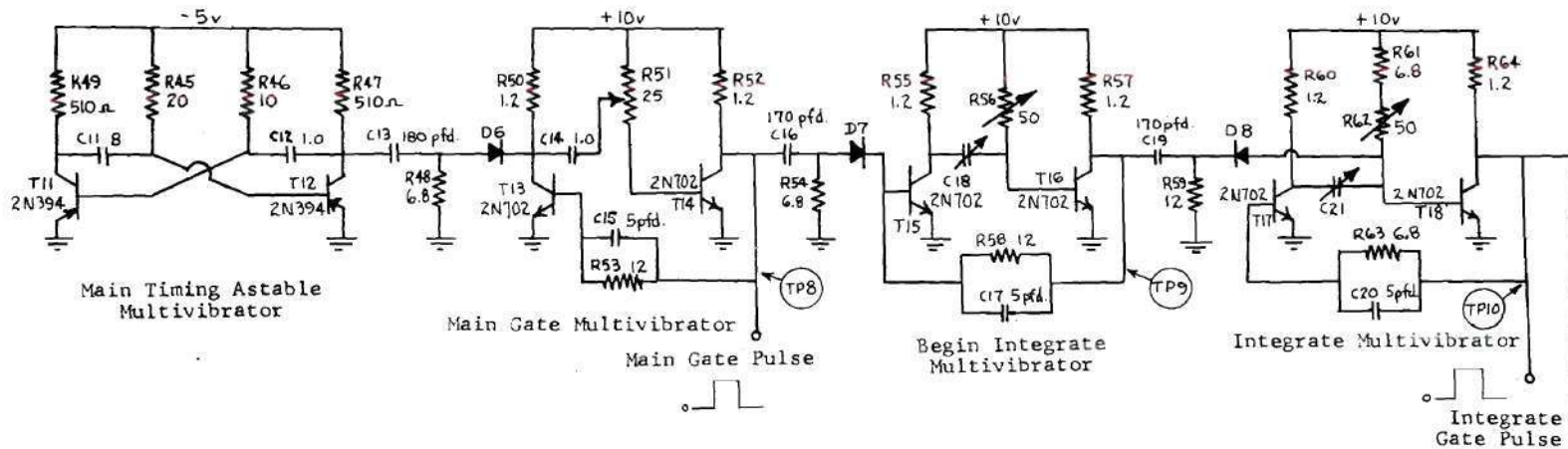


Figure A8. Schematic Diagram of the Simulated Receiver Excluding Timing Circuitry.



Notes:

1. All capacitances are in microfarads and all resistances are in kilohms unless otherwise shown. All diodes are 1N97.
2. Capacitors C18 and C21 are each selected from among 0.002, 0.0033, 0.0068, 0.012, 0.027, 0.047, 0.1, 0.2, and 0.4 microfarads by separate front panel rotary switches. The C2 rotary switch is in tandem with the C1 rotary switch described in the preceding figure.
3. Test points shown (TP *) are brought out to chassis jacks.

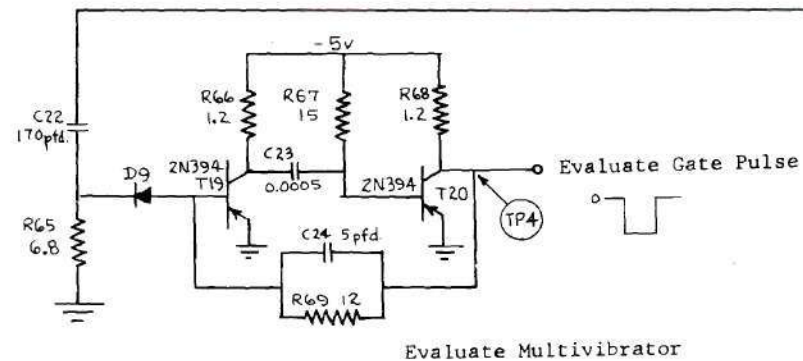


Figure A9. Schematic Diagram of the Simulated Receiver Timing Circuitry.

BIBLIOGRAPHY

1. Schwartz, Mischa, Information Transmission, Modulation and Noise, McGraw-Hill Book Company, Inc., New York, 1959, p. 400.
2. Middleton, "Some General Results in the Theory of Noise Through Non-Linear Devices," Quarterly of Applied Mathematics, Vol. 5, No. 4, pp. 470, 471, January 1948.
3. Kac, M. and Siegert, A. J. F., "On the Theory of Noise in Radio Receivers with Square Law Detectors," Journal of Applied Physics, Vol. 18, No. 4, pp. 383-397, April 1947.
4. Meyer, M. A. and Middleton, David, "On the Distribution of Signals and Noise after Rectification and Filtering," Journal of Applied Physics, Vol. 25, No. 8, August 1954.
5. Emerson, R. C., "First Probability Densities for Receivers with Square-Law Detectors," Journal of Applied Physics, Vol. 24, No. 9,
6. Middleton, David, Introduction to Statistical Communication Theory, McGraw-Hill Book Company, Inc., New York, 1960, p. 147.
7. Marcum, J. I., "A Statistical Theory of Target Detection by Pulsed Radar: Mathematical Appendix," I.R.E. Transactions on Information Theory, April 1960.
8. Middleton, Ibid.
9. Lee, Y. W., Statistical Theory of Communication, John Wiley and Sons, Inc., New York, 1960, pp. 268-272.
10. Reference Data for Radio Engineers, Fourth Edition, International Telephone and Telegraph Company, 1956, p. 23.
11. Terman, F. E., Electronic and Radio Engineering, Fourth Edition, McGraw-Hill Book Company, Inc., New York, 1955, pp. 547-557.
12. Marcum, Ibid., p. 189.
13. Middleton, David, Ibid.
14. Strauss, Leonard, Wave Generation and Shaping, McGraw-Hill Book Company, Inc., New York, 1960, Chapters 9 and 10.